WP 2004-5

Higher-Order Finite Element Solutions of Option Prices

by

Peter Raahauge

INSTITUT FOR FINANSIERING, Handelshøjskolen i København
Solbjerg Plads 3, 2000 Frederiksberg C
tlf.: 38 15 36 15 fax: 38 15 36 00

DEPARTMENT OF FINANCE, Copenhagen Business School
Solbjerg Plads 3, DK - 2000 Frederiksberg C, Denmark
Phone (+45)38153615, Fax (+45)38153600
www.cbs.dk/departments/finance

ISBN 87-90705-81-5
ISSN 0903-0352

HIGHER-ORDER FINITE ELEMENT SOLUTIONS OF OPTION PRICES

Peter Raahauge*
Department of Finance
Copenhagen Business School

September 9, 2004

Kinks and jumps in the payoff function of option contracts prevent an effective implementation of higher-order numerical approximation methods. Moreover, the derivatives (the *greeks*) are not easily determined around such singularities, even with standard lower-order methods. This paper suggests a transformation to turn the original ill-conditioned pricing problem into a well-behaved numerical problem. For a standard test case, both vanilla- and binary call price functions are approximated with (tensor) B-splines of up to 10'th order. Polynomial convergence rates of orders up to approximately 10 are obtained for prices as well as for first and second order derivatives (delta and gamma). Unlike similar studies, numerical approximation errors are measured both as weighted averages and in the supnorm over a state space including time-to-maturities down to a split second.

KEYWORDS: Numerical option pricing, Transformed state spaces, Higher-order B-splines.

1. INTRODUCTION

Many financial option contracts of both academic and practical interest do not have known closed form price solutions and prices must be found by numerical methods. But most option contracts have singularities in the payoff function. As noted by Heston and Zhou (2000), this implies that the usual theorems of standard numerical analysis are not applicable to interesting option pricing problems in finance. Despite the fact that the option price function is mostly well-behaved prior to maturity, the singularities prevent an effective implementation of higher-order numerical methods. Instead, lower-order (usually linear) methods with at most quadratic convergence order, $\mathcal{O}(N^{-2})$, are common. This paper suggests a method to effectively apply higher-order methods with convergence rates of up to 10'th order, $\mathcal{O}(N^{-10})$.

A number of remedies to deal with the effects of singularities in option payoff functions have already been suggested. The focus has been to secure smooth quadratic convergence of standard methods, not to facilitate methods with higher convergence rates.

Kreiss, Thomée, and Widlund (1970) and Thomée and Wahlbin (1974) analyzed in a general setting a simple method for smoothing the initial conditions for parabolic problems by replacing the true initial condition with an average of surrounding values. The

*I would like to thank Carsten Sørensen for comments.

method has been studied in an option pricing setting by Heston and Zhou (2000), Tavella and Randall (2000), and Pooley, Vetzal, and Forsyth (2003). In a binomial setting Heston and Zhou (2000) finds that for vanilla[1] European and American calls averaging the payoff provide a more smooth convergence that allows for extrapolation. The findings show that the averaging method in itself does not reduce the approximation errors. In a traditional finite difference (FD) setting, Tavella and Randall (2000, chap. 4) investigates the effect of averaging payoffs for European type options with vanilla- and binary call payoff functions. The results for the vanilla call are in accordance with the findings of Heston and Zhou (2000). For the binary payoff, the averaging method is found to increase the convergence rate. Although some smoothing of the convergence is obtained, it is not enough to allow for extrapolation techniques. In a linear finite element (FE) setting Pooley, Vetzal, and Forsyth (2003) investigates European-type options with binary- and supershare binary call payoffs, and the findings are in accordance with the results in Tavella and Randall (2000, chap. 4). In addition to the averaging method, a mixture of implicit and Crank-Nicolson time-stepping, suggested by Rannacher (1984), is implemented and smooth convergence is obtained for even binary payoffs.

Somewhat related to the averaging method is the method of "grid positioning" investigated by Tavella and Randall (2000, chap. 5). By choosing the grid points of the numerical approximation such that the exercise price falls exactly on a grid point for vanilla options and exactly in the middle of two grid points for binary options, results similar to the ones of the averaging method are obtained. Again, Pooley, Vetzal, and Forsyth (2003) finds that the "Rannacher time-stepping" is necessary for smooth convergence in the binary case.

A more general projection method has been suggested by Rannacher (1984) and investigated in connection with binary option payoffs by Pooley, Vetzal, and Forsyth (2003). Also, Heston and Zhou (2000) suggest to combine numerical solutions with approximating closed form solutions for short maturities. Both suggestions provide results similar to the results of the averaging method and the grid positioning method.

This paper differs from the previous studies in three important ways. First, the existing studies do not change the fact that an approximation of the option price function is an ill-conditioned numerical problem near the singularity points. The various remedies help linear methods to achieve a quadratic convergence rate, but it is not clear to what extend they facilitate methods with higher convergence rates. On the contrary, the transformation method suggested below replaces the original problem with a well-behaved numerical problem with moderate derivatives. Intuitively, the singularity point is stretched to a line, and exact smooth initial value conditions are obtained from closed form solutions of the limiting heat equation. Higher order finite element methods (B-splines) of orders up to 10 are applied to pricing problems were kinks (vanilla calls) and jumps (binary calls) have been smoothed by the transformation. The expected potential of the higher-order methods is reached and polynomial convergence rates of order 10, $\mathcal{O}(N^{-10})$, are obtained. As a result, the precision of the price approximation obtained with higher-order methods using 400 parameters determined by a sparse linear equation system dominates the precision of traditional smoothing methods based on more than 10 million parameters.

Second, the existing studies of singularity remedies measure the numerical approximation error for a single option price only: An at-the-money option with six months or

[1]Below, "vanilla" characterizes options with payoff functions of the form $\max(S_t - x, 0)$ or $\max(x - S_t, 0)$ were S_t is the underlying asset price and x the exercise price.

12 months to maturity. Since the numerical difficulties are located immediately before maturity, the analysis below measures the errors more broadly over the state space. The supnorm reports the error level for the areas of the state space where the numerical approximation is least effective. The weighted average norm provides some information on the expected pricing error regardless of time to maturity and price of the underlying asset. An example shows that the pricing error of a binary option with six months to maturity might not have the same asymptotic convergence rate as the average price error.

Third, despite significant practical importance for hedging purposes, the precision of first- and second order derivatives with respect to the underlying asset price (delta and gamma) has received little attention by the studies reported above. Below, convergence rates and error levels for delta and gamma are reported in terms of both weighted averages and supnorm. The results match the $\mathcal{O}(N^{-10})$-convergence of the price function. As a result, 400 parameter solutions of even binary options provide very accurate approximations of delta and gamma as close as 0.001 seconds before maturity. For binary options traditional methods converge neither in the supnorm nor in the average.

In Section 2 it is argued that for a general class of underlying price processes, the partial differential equation (PDE) describing option prices converges to a heat equation near a singularity point. Based on the nature of the closed form heat equation solutions, the appropriate transformation is suggested and a smooth initial condition for the transformed problem is provided. Section 3 and 4 investigates the effectiveness of the transformation for a vanilla call and a binary call in the familiar Black-Scholes setup. Section 3 implements a time-dependent FE approximation (hybrid FE/FD) where the solution in the time-dimension is FD approximated and the solution in the asset price dimension is approximated with B-splines from cubic to 10'th order. Section 4 implements a full FE approximation using two-dimensional tensor B-splines. Section 5 concludes.

In Section 2 it is argued that for a general class of underlying price processes, the partial differential equation (PDE) describing option prices converges to a heat equation near a singularity point. Based on the nature of the closed form heat equation solutions, the appropriate transformation is suggested and a smooth initial condition for the transformed problem is provided. Section 3 and 4 investigates the effectiveness of the transformation for a vanilla call and a binary call in the familiar Black-Scholes setup. Section 3 implements a time-dependent FE approximation (hybrid FE/FD) where the solution in the time-dimension is FD approximated and the solution in the asset price dimension is approximated with B-splines from cubic to 10'th order. Section 4 implements a full FE approximation using two-dimensional tensor B-splines. Section 5 concludes.

2. The Transformation of the State Space

Below, the option price of interest, U, is a function of time, t, and the price of a single underlying asset, S_t. Like Pooley, Vetzal, and Forsyth (2003), the analysis will focus on European type options with piecewise linear payoff functions at maturity ($t = T$) of the contract. Both kinks (vanilla options) and jumps (binary options) are considered. Only payoffs with one singularity are considered. Little generality is lost, however, since options with more than one payoff singularity might be considered as a sum of simpler options with only one singularity point each. Let $(S_t, t) = (x, T)$ be the singularity point

of interest, where x is known as the exercise price.

2.1. THE LIMITING HEAT EQUATION

The price of the underlying asset is assumed to follow a general stochastic differential equation of the form

$$dS_t = \mu(S_t, t)dt + \sigma(S_t, t)dw_t \tag{1}$$

where w_t is a standard Brownian motion and μ and σ are known functions. Under standard regularity conditions, especially continuity of μ, σ, and r, the option price solves the familiar PDE:

$$r(S_t, t)U(S_t, t) = \frac{\partial U}{\partial t} + r(S_t, t)S_t\frac{\partial U}{\partial s} + \tfrac{1}{2}\sigma(S_t, t)^2\frac{\partial^2 U}{\partial S^2}, \tag{2}$$

where r is the riskfree rate of the economy and the particular solution is determined by boundary conditions and the initial conditions $U(S_T, T)$.

To ease the notation, t is replaced by time-to-maturity, $\tau = T - t$. Moreover, $r_\tau = r(S_t, t)$ and $\sigma_\tau = \sigma(S_t, t)$, $\tau > 0$ are used with the dependence of S_t left implicit. At maturity, the notation $r_0 = r(x, T)$ and $\sigma_0 = \sigma(x, T)$ is used. I.e., at maturity, the shorthand notation is valid for the singularity point only. Finally, a standard forward price transformation using the singularity point interest rate r_0 is applied,

$$\begin{aligned} s_\tau &= S_t e^{r_0\tau}, \\ u(s_\tau, \tau) &= U(S_t, t)e^{r_0\tau} \end{aligned}$$

in order to rewrite (2) to

$$(r_\tau - r_0)u = -\frac{\partial u}{\partial \tau} + (r_\tau - r_0)s_\tau\frac{\partial u}{\partial s} + \tfrac{1}{2}\sigma_\tau^2\frac{\partial^2 u}{\partial s^2}e^{2\,r_0\tau}. \tag{3}$$

Consider the limit form of (3) when approaching the singularity point, $(s_\tau, \tau) \to (x, 0)$:

$$\frac{\partial u}{\partial \tau} = \tfrac{1}{2}\sigma_0^2\frac{\partial^2 u}{\partial s^2}, \tag{4}$$

which is the well-known heat equation. Since $u \to U$ and $s \to S$ for $\tau \to 0$, the closed form solutions to the heat equation provides information on how option prices behave near the singularity point.

2.2. THE FUNDAMENTAL SOLUTION

The solution to the heat equation in (4) depend on the initial condition. Since the solutions for all initial conditions can be expressed on the basis of the *fundamental solution*, this solution is considered first. Assume that the initial condition $u(s_0, 0)$ is the Dirac function with $s_0 - x$ as argument: $\delta(s_0 - x)$.[2] The solution to (4) is then given by the fundamental solution (Green's function):

[2]The Dirac function integrates to one, but have mass only at zero.

$$G(s_\tau, \tau; x) = \frac{1}{\sqrt{2\pi\tau\sigma_0^2}} e^{-\frac{1}{2}\left(\frac{s_\tau - x}{\sqrt{\tau}\sigma_0}\right)^2}, \qquad \tau > 0, \tag{5}$$

with $G = \delta$ for $\tau = 0$, see e.g. Wilmott, Dewynne, and Howison (1993). Note that G is singular at $(s_\tau, \tau) = (x, 0)$. Define the following variable,

$$m_\tau = \frac{s_\tau - x}{\sigma_0\sqrt{\tau}}, \tag{6}$$

which is called the *volatility-adjusted moneyness* below. With this definition, the fundamental solution can be expressed in terms of m_τ instead of s_τ:

$$\begin{aligned} G(m_\tau, \tau) &= \frac{1}{\sqrt{\tau}} \frac{\varphi(m_\tau)}{\sigma_0} \\ &= g(\tau) f_0(m_\tau) \end{aligned} \tag{7}$$

where φ denote the standard normal probability density function, $g(\tau) = \tau^{-0.5}$, and $f_0(m_\tau) = \varphi(m_\tau)/\sigma_0$. The subscript on f_0 indicates that for option pricing problems in general where $r_\tau \neq r_0$ and $\sigma_\tau \neq \sigma_0$, $\tau > 0$, the function applies in the limit only.

Equation (7) suggests three important general properties on which the idea of the paper rests. First, the decomposition into a τ-dependent part and an m_τ-dependent part is useful form a numerical point of view since it allows to single out the ill-conditioned dependence of τ into an explicit part g which need no numerical approximation. Instead, the numerical work will focus on determining the remaining part of the price expression.

Second, note that f_0 is well behaved from a numerical point of view with small derivatives up to high orders. Outside the heat equation setting, closed form solutions will not in general be available and the function will not be time-independent: $f = f(m_\tau, \tau)$. However, if r_τ and σ_τ are smooth functions, it is reasonable to expect that f will inherit the well-behaved derivatives of the limiting solution f_0. If this is so, powerful higher-order approximation methods come into play.

Third, regular state spaces seem more efficient when based on m_τ instead of s_τ. In a numerical implementation, artificial state space boundaries must be introduced, $s_\tau \in [\underline{s},\ \overline{s}]$. The location of these bounds must be chosen based on a trade off. If $\underline{s}$ and $\overline{s}$ are chosen too close to x, the truncation error caused by the artificial bounds will be high. If the bounds are chosen too far from x, the numerical price approximation will have to span an unnecessary large state space and the quality of the numerical solution will be low.

In order to define a criteria for locating the boundaries, let $|G(s_\tau, \tau) - G(s_\tau, 0)|$ denote the *time effect* and let the cumulative time effect up to $\tilde{s}$ at time τ be given by

$$E(\tilde{s}, \tau) = \int_{-\infty}^{\tilde{s}} |G(s, \tau) - G(s, 0)| ds.$$

I.e., $E(\tilde{s}, \tau)$ reflects the difference between the price at τ and the initial value when measured over the interval $]\infty, \tilde{s}]$. Consider now the following criteria for determining the lower boundary of the state space $\underline{s}$,

$$\frac{E(\underline{s}, \tau)}{E(\infty, \tau)} = \alpha, \qquad 0 < \alpha < 1$$

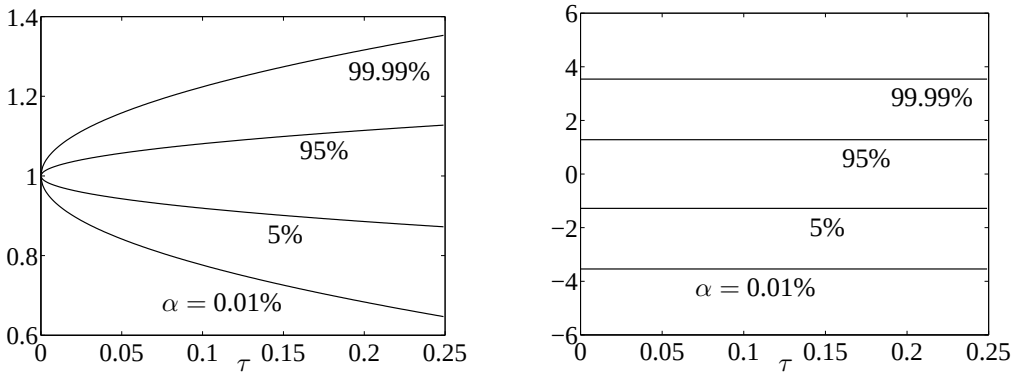

(a) $\underline{s}$ for selected α-values

(b) $\underline{m}$ for selected α-values

Figure 1: Cumulative effect of $\delta(S_\tau - x)$
x = 1, $\sigma_0 = 0.2$

where $E(\infty, \tau)$ denote the entire time effect and α is the ratio of time effect that is truncated due to the artificial lower boundary. By choosing α it is possible to control how much of the time effect is lost when the boundaries are introduced. If, for instance, $\alpha = 0.01$, the truncation error loss is 1%. For the fundamental solution, this criterium gives the following lower boundary:

$$\Phi\left(\frac{\underline{s} - x}{\sigma_0\sqrt{\tau}}\right) = 2\alpha. \tag{8}$$

where Φ denote the standard normal probability distribution function. Equation (8) shows that the lower boundary in terms of s_τ will be time dependent. Such boundaries are shown in Figure 1(a) for various choices of α. The figure shows that the traditional practice of choosing a constant lower bound in the s-space might result in an approximation space too wide for short maturities and too narrow for long maturities. If, however, boundaries are represented in terms of volatility-adjusted moneyness, equation (8) gives the condition

$$\Phi(\underline{m}) = 2\alpha$$

which clearly results in a time-independent lower bound. Figure 1(b) shows the same bounds as 1(a) but in terms of m_τ rather than s_τ. Since the bounds are linear, a regular state space with constant boundaries can be chosen while maintaining a fixed truncation error for all maturities. As show in Appendix D this property carries over to the payoff functions considered below.

Based on the three properties listed above, the following approach for determining numerical option prices is suggested:

A For the relevant option payoff function, determine the solution to the limiting heat equation at the singularity point and decompose like in (7) the solution into a τ-dependent part, g, (for which the functional form is known) and an m - dependent part, f_0.

B Transform the original PDE in (2) into an equivalent PDE with m_τ as state variable instead of s_τ.

C Determine a numerical solution to f according to the transformed PDE with the closed form f_0-solution from point B as the initial condition.

In Section 2.3 and 2.4 below, step A and B are show for vanilla- and binary call options defined on prices following the general partial differential equation in (1). In Section 3 and 4 step C is investigated for the familiar special case with log-normal asset price process (the Black-Scholes setup).

2.3. Initial Conditions for Options

For obvious reasons, no derivatives promise a payoff equal to a Dirac function. However, the fundamental solution can be used to derive heat equation solutions for general payoff functions. Let $u(s_0, 0)$ denote the payoff function of the option of interest. Then, the price function is determined by

$$u(s_\tau, \tau) = \int u(s, 0) G(s, \tau; s_\tau) ds, \qquad \tau > 0, \tag{9}$$

see, e.g., Wilmott, Dewynne, and Howison (1993). For piecewise linear payoff functions, the closed form solutions are easily determined. For the initial condition of a vanilla call option, $u(s_0, 0) = \max(s_0 - x, 0)$, equation (9) gives the price function

$$u(s_\tau, \tau) = \sqrt{\tau}\, \sigma_0 \left(m_\tau \Phi(m_\tau) + \phi(m_\tau) \right), \tag{10}$$

see Appendix B. As for the fundamental solution, the solution decomposes into a time-dependent part, $g(\tau) = \sqrt{\tau}$, and a m-independent part, $f_0(m_\tau) = \sigma_0(m_\tau \Phi(m_\tau) + \phi(m_\tau))$, which is well-behaved in terms of derivatives with respect to m_τ.

Along the same lines the limiting heat equation solution for the binary call payoff function, $u(s_0, 0) = \mathcal{H}(s_0 - x)$,[3] is obtained,

$$u(s_\tau, \tau) = \Phi(m_\tau). \tag{11}$$

Since the solution shows no dependence of time, for fixed m_τ, there is no need for factorization into separate terms in the binary case: $g(\tau) = 1$ and $f_0(m_\tau) = \Phi(m_\tau)$. As before, the derivatives up to high orders are of moderate size.

2.4. Transformation of the PDE

Based on the arguments so far, let the price function be decomposed according to

$$U(S_t, t) = g(\tau) f(m_\tau, \tau) e^{r_0 \tau}$$

where $g(\tau)$ is known and f it to be determined. Based on the original PDE in (2), Appendix E.1 shows that f is determined by the following transformed PDE:

$$(\tau \Delta r + \gamma) f = -\tau \frac{\partial f}{\partial \tau} + \left(\left(\tau \Delta r + \tfrac{1}{2} \right) m_\tau + \sqrt{\tau} \frac{\Delta r x}{\sigma_0} \right) \frac{\partial f}{\partial m} + \tfrac{1}{2} \frac{\sigma_\tau^2}{\sigma_0^2} \frac{\partial^2 f}{\partial m^2} e^{2 r_0 \tau}, \tag{12}$$

[3] $\mathcal{H}(x)$ is the Heaviside function equal to one for $x \geq 0$ and zero otherwise.

where $\Delta r = r_\tau - r_0$ and $\gamma = \tau(\partial g/\partial \tau)/g$. Note that in the vanilla call case $\gamma = 1/2$ whereas the case of a binary call gives $\gamma = 0$.

The PDE in (12) involves $\sqrt{\tau}$-terms which, from a numerical point of view, is not attractive. Therefore, a transformation of time might be considered:

$$\theta = \sqrt{\tau}.$$

Appendix E.2 shows that in this case, f must solve the following PDE:

$$(\theta^2\Delta r + \gamma)f = -\frac{\theta}{2}\frac{\partial f}{\partial \theta} + \left((\theta^2\Delta r + \tfrac{1}{2})m_\theta + \theta\frac{\Delta r x}{\sigma_0}\right)\frac{\partial f}{\partial m} + e^{2r_0\theta^2}\frac{\sigma_\tau^2}{2\sigma_0^2}\frac{\partial^2 f}{\partial m^2}. \tag{13}$$

It is easily verified that the solution to the limiting heat equation for the vanilla call in (10) and the binary call in (11) are valid solutions to limiting versions of (12) and (13). For the vanilla call both (12) and (13) converges to

$$f = m_\tau\frac{\partial f}{\partial m} + \frac{\partial^2 f}{\partial m^2}$$

for $(s_\tau, \tau) \to (x, 0)$. The binary call PDE's have the same limit form except that the left hand side is equal to zero instead of f.

As an alternative to the variable-transformation of the PDE, an index form of the original PDE in (2) might be considered, see Tavella and Randall (2000, p. 160). However, for the transformation above, the functional relationship between the stock price and moneyness degenerates for $\tau \to 0$. As a result, the initial condition contains little information and the quality of the numerical solutions close to the point $(S_\tau, \tau) = (x, 0)$ will decrease significantly. In this case, improvements can be made by following Heston and Zhou (2000) and start the approximation at a small $\tau > 0$ and use closed form approximations (the Black-Scholes price) as the "initial" condition. Further improvements might be obtained using *Rannacher timestepping* as implemented by Pooley, Vetzal, and Forsyth (2003).

2.5. Alternative Moneyness-definitions

Based on the fundamental solution of the limiting heat equation, the m_τ-definition used above suggests itself. However, the definition suffers from a serious drawback in a financial setting if a regular state space with a fixed lower boundary $\underline{m}$ is wanted for long maturity options. According to the m_τ-definition used, the implicit lower boundary of the stock price,

$$\underline{s} = (1 + \sigma_0\sqrt{\tau}\,\underline{m})x,$$

decreases with the maturity and falls below zero eventually. Such problems are avoided with another definition of volatility-adjusted moneyness where constant boundaries are better suited for standard asset price processes. One such definition could be

$$n_\tau = \frac{\log(s_\tau/x)}{\sigma_0\sqrt{\tau}}$$

in which case the stock price will always be non-negative for $n_\tau \in \mathbb{R}$,

$$s_\tau = \left(e^{\sigma_0\sqrt{\tau}\,n_\tau} - 1\right) x.$$

Another moneyness-definition affects the PDE for f as well as the initial condition, see Appendix F. Since the options analyzed below have a time-to-maturity not longer than six months, the original moneyness definition in (6) will be used throughout.

2.6. The Black Scholes Case

The most familiar specification of the stochastic differential equation in (1) is the Black-Scholes specification,

$$dS_t = \mu S_t dt + \sigma S_t dw,$$

where σ is a constant. Hence, in terms of the notation above, $\sigma_\tau = \sigma S_\tau$ and $\sigma_0 = \sigma x$. The assumption of a constant asset price growth rate is accompanied by an assumption of a constant interest rate r. In the Black-Scholes case the PDE in (12) simplifies to

$$\gamma f = -\tau\frac{\partial f}{\partial \tau} + \tfrac{1}{2} m_\tau \frac{\partial f}{\partial m} + \tfrac{1}{2}(1+\sqrt{\tau}\sigma m_\tau)^2 \frac{\partial^2 f}{\partial m^2}. \tag{14}$$

The time-transformed PDE in (13) simplifies to a similar form without any square-root elements,

$$\gamma f = -\tfrac{1}{2}\theta\frac{\partial f}{\partial \theta} + \tfrac{1}{2} m_\theta \frac{\partial f}{\partial m} + \tfrac{1}{2}(1+\theta\sigma m_\theta)^2 \frac{\partial^2 f}{\partial m^2}. \tag{15}$$

The initial conditions in (10) and (11) are, of course, valid for the Black-Scholes case also, since the limiting PDE in (14), like the more general PDE in (12), converges to the relevant heat equation PDE. Note that in the Black-Scholes case, the volatility-adjusted moneyness

$$m_\tau = \frac{1}{\sigma\sqrt{\tau}}\frac{s_\tau - x}{x}$$

might be given a return interpretation as $(s-x)/x$ can be interpreted as the asset return necessary for the option be be at-the-money at maturity and $\sigma\sqrt{\tau}$ is the volatility of this return.[4]

Figure 2(a) and 2(b) provide some insight into how well the properties of the f_0-function are inherited by the f-function in the Black-Scholes case. The Limit-functions are the f_0-functions from (10) and (11) respectively. From the figures it is clear that $f \to f_0$ for $\tau \to 0$. Note, however, that even for prices with half a year to maturity the deviation from the initial condition is quite small. This suggests that besides the time-factor of g, the option prices are almost constant in m_τ.

3. Time-dependent Finite Element Approximations

The next two sections investigate the effectiveness of higher-order B-splines as basis functions in a FE solution procedure for f in the Black Scholes setup. The first section

[4]The analogy is not perfect as the interpretation mixes continuous and discrete compounding. This is not the case for the alternative moneyness definition suggested in Section 2.5.

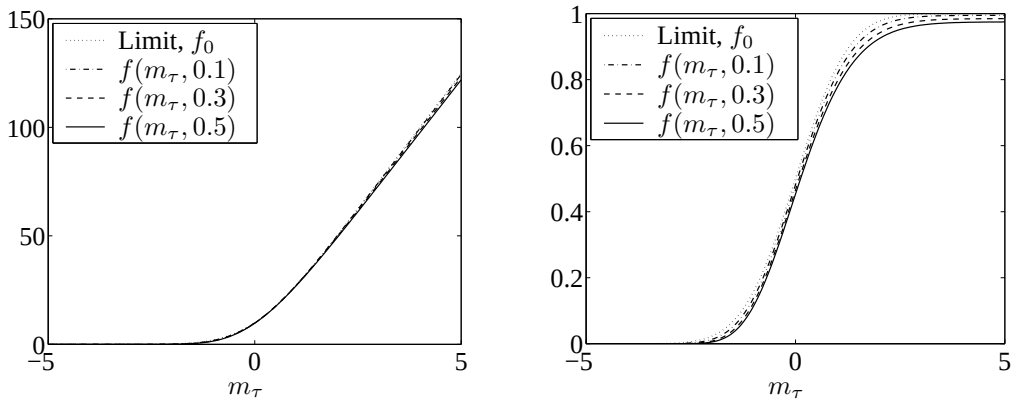

(a) Vanilla Call (b) Binary Call

Figure 2: Option prices in m_τ

The f-part of the price (determined as u/g) is shown, were u is the Black Scholes formula price except for the "limit" were the heat equation solution is used. For the vanilla call, $g(\tau) = \sqrt{\tau}$ were used. For the binary call, no time-adjustment were used, $g(\tau) = 1$. For both options $x = 100$, $r = 0.03$, and $\sigma = 0.25$.

investigates a time-dependent FE (or hybrid FE/FD) procedure. This procedure approximates f at maturity and works itself backwards by approximating f successively for larger and larger τ-values. Time-derivatives are determined by a FD approach.

3.1. The one-dimensional B-spline Basis

The choice of basis-functions is important for a successful implementation of a finite element procedure. The most popular choice in option pricing is a piecewise linear basis, e.g., Zvan, Forsyth, and Vetzal (1998b, 1998b, 1999, 2000, 2001), Forsyth, Vetzal, and Zvan (1999), Pooley et al. (2000), and Barone-Adesi, Bermudez, and Hatgioannides (2003). Note that the widely used FD-methods can be seen as special cases of piecewise linear FE methods. Quadratic and cubic methods have been considered, e.g. Jackson and Süli (1998) and Lai and Wong (2004), as well as higher-order explicit methods, e.g. Heston and Zhou (2000), but convergence rates beyond quadratic are note reported for actual implementations.

For the well-behaved problem of approximating f, higher-order methods should be considered. One possibility is orthogonal global polynomials but for many option payoffs this choice might not be appropriate as the price function is linear at the endpoints of the approximation whereas significant curvature is located at the interior. Moreover, global polynomials are expensive to work with from a computational point of view. Instead, B-splines are considered below.

For a given τ, a FE-approximation of the option price is wanted over the relevant moneyness interval, $[\underline{m},\ \overline{m}]$. To define a B-spline basis of order K,[5] a sequence of equally spaced knots $M = \{m^1, m^2, \ldots, m^{N+1}\}$, $m^1 = \underline{m}$ and $m^{N+1} = \overline{m}$, is used. With proper multiplicities K at the endpoints, this sequence defines the B-spline basis functions, $B^n(m_\tau),\ m_\tau \in [\underline{m},\ \overline{m}],\ n \in \{1, 2, \cdots N + K - 1\}$, where the dependence of M

[5]The polynomial $\alpha_1 + \alpha_2 x + \cdots + \alpha_K x^{K-1}$ is said to be of order K.

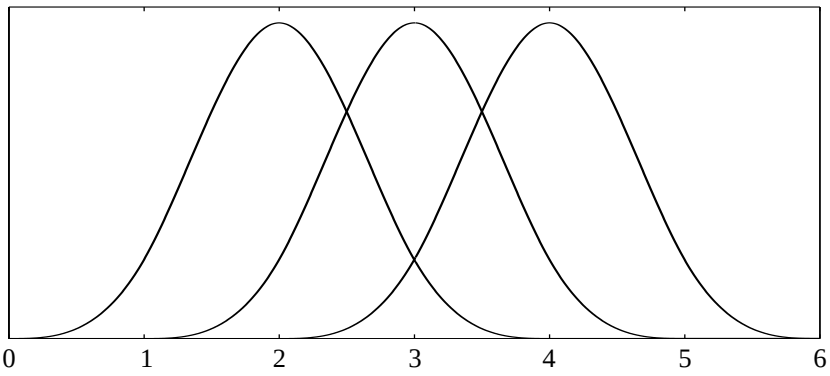

FIGURE 3: Three cubic B-splines

and K is suppressed by the notation.[6] Let $B(m_\tau)$ denote the row vector of basis splines:

$$B(m_\tau) = \left[B^1(m_\tau)\ B^2(m_\tau)\ \ldots\ B^{N+K-1}(m_\tau)\right].$$

The full approximation is a linear function of the individual B-spline values for a given point,

$$f(m_\tau, \tau) \approx B(m_\tau, a_\tau) = B(m_\tau)a_\tau$$

where $a = [a^1, a^2, \ldots, a^{N+K-1}]^\top$ is a column vector of free parameters determining the approximation and the subscript is used to indicate for which τ the approximation is relevant. Note that the approximation only depends on τ via the parameters since the basis functions are constant through time. The approximation spans the space of piecewise polynomials of order K with continuous $K-2$ order derivatives at the knots. Figure 3 shows cubic B-splines ($K = 4$) defined over integer knots.

The one-dimensional B-spline approximation will be calculated for a finite number of maturities, $\tau \in \Theta = \{\tau^1, \tau^2, \ldots, \tau^{J+1}\}$, with $\tau^1 = 0$. At τ^1, f is determined by the initial condition f_0. Then, approximations are calculated for $\tau^2, \tau^3, \ldots$ recursively based on the relevant PDE.

3.2. DERIVATIVES

To approximate the relevant PDE, derivatives of $B(m_\tau, a_\tau)$ are needed. Since the approximation is a linear function of polynomials, derivatives with respect to m_τ are easily available. Let $B_m^n(m_\tau)$ denote the first order derivatives of the n'th B-spline, and let $B_m(m_\tau)$ denote the corresponding vector of derivatives. The first order derivative of the approximation is then $B_m(m_\tau, a_\tau) = B_m(m_\tau)a_\tau$. The second order derivative $B_{mm}(m_\tau, a_\tau) = B_{mm}(m_\tau)a_\tau$ is obtained similarly. In order to improve the stability of the approximation scheme, it is customary to let the approximation of $\partial f/\partial m$ be a weighted average of $B_m(m_\tau)a_\tau$ and $B_m(m_\tau)a_{\tau'}$, where $\tau' \in \Theta$ is the immediate predecessor to τ in Θ, $\tau' < \tau$. Hence,

[6] See Judd (1998) for an introduction or de Boor (1978) for a fuller treatment of B-splines.

$$\frac{\partial f}{\partial m_\tau} \approx \omega B_m(m_\tau)a_\tau + (1-\omega)B_m(m_\tau)a_{\tau'}$$

and similarly for f_{mm}

$$\frac{\partial^2 f}{\partial m^2} \approx \omega B_{mm}(m_\tau)a_\tau + (1-\omega)B_{mm}(m_\tau)a_{\tau'}$$

where $0 \leq \omega \leq 1$. Implementations base on values of ω equal to 0, 1, and $1/2$ respectively are known as the explicit-, the implicit-, and the Crank-Nicolson method, respectively.

Since the approximation is discrete in the time-dimension, a finite difference approach must be used for time derivatives. The following standard non-central approximation is used for the time derivative.

$$\frac{\partial f}{\partial \tau} \approx \frac{B(m_\tau)a_\tau - B(m_\tau)a_{\tau'}}{\Delta\tau}$$

where $\Delta\tau = \tau - \tau'$ and $a_{\tau'}$ will be fixed when a_τ is determined.

3.3. THE PDE-APPROXIMATION

With the coefficients β defined according to either (12) or (13), the relevant PDE can be expressed in a more compact form:

$$\beta_0 f = -\beta_1 \frac{\partial f}{\partial \tau} + \beta_2 \frac{\partial f}{\partial m} + \beta_3 \frac{\partial^2 f}{\partial m^2}.$$

With the definitions of the derivatives above, the numerical approximation to this equation, for a given point (m_τ, τ), is given by

$$A(m_\tau, \tau)a_\tau = C(m_\tau, \tau)a_{\tau'} \tag{16}$$

where

$$A(m_\tau, \tau) = (\beta_0 + \beta_1/\Delta\tau)B(m_\tau) - \omega\beta_2 B_m(m_\tau) - \omega\beta_3 B_{mm}(m_\tau)$$

and

$$C(m_\tau, \tau) = (\beta_1/\Delta\tau)B(m_\tau) - (1-\omega)\beta_2 B_m(m_\tau) - (1-\omega)\beta_3 B_{mm}(m_\tau).$$

Note that the equation is a linear function of the parameters a_τ and a'_τ. Although the approximation basis is constant, both A and C generally depend on τ via the β-coefficients.

APPROXIMATION CRITERIA

The $N + K - 1$ parameters in a_τ are determined by interpolation at the interior knots in M as well as boundary conditions. Accordingly, $N - 1$ parameters are determined by requiring (16) to hold with equality for $m_\tau \in \{m^2, \ldots, m^N\}$. With the interpolation points fixed, define the following matrices of stacked interpolation condition row vectors:

$$\mathbb{A}(\tau) = \begin{bmatrix} A(m^2,\tau) \\ \vdots \\ A(m^N,\tau) \end{bmatrix} \qquad \mathbb{C}(\tau) = \begin{bmatrix} C(m^2,\tau) \\ \vdots \\ C(m^N,\tau) \end{bmatrix}$$

In order to impose the boundary conditions, define $\hat{f}$ as the f-equivalent to the *internal value* of the options. For the vanilla call,

$$\begin{aligned} & g(\tau)\hat{f}(m_\tau,\tau)e^{-r_0\tau} = \max(S_t - x^{-r_0\tau}, 0) \\ (17) \qquad & \Downarrow \\ & \hat{f}(m_\tau,\tau) = \max\left(\sigma x m_\tau, 0\right), \qquad \text{since } \; g(\tau) = \sqrt{\tau}. \end{aligned}$$

Similar for the Binary call,

$$(18) \qquad \hat{f}(m_\tau,\tau) = \mathcal{H}(m_\tau), \qquad \text{since } \; g(\tau) = 1.$$

Note that the notation below reflects the fact that $\hat{f}$, as seen from (17) and (18) is time-independent in both cases when m_τ is used as state variable. At the boundaries the approximation as well as its derivatives will be determined by $\hat{f}$ in order to restrict the remaining K parameters,

$$(19) \qquad \begin{aligned} B_{i\cdot m}(\underline{m})a_\tau &= \hat{f}_{i\cdot m}(\underline{m}) = \left.\frac{\partial^i \hat{f}}{\partial m^i}\right|_{m_\tau=\underline{m}} \\ B_{i\cdot m}(\overline{m})a_\tau &= \hat{f}_{i\cdot m}(\overline{m}) = \left.\frac{\partial^i \hat{f}}{\partial m^i}\right|_{m_\tau=\overline{m}} \end{aligned} \qquad i = 0,1,\ldots,I = \frac{K-2}{2}$$

where $B_{0\cdot m}(m_\tau)$ and $\hat{f}_{0\cdot m}(m_\tau)$ is a convenient notation for the level of the two functions. For the case of $K = 4$, for instance, these restrictions result in the Hermite cubic spline. Since $\hat{f}$ is linear, second- and higher order derivatives are restricted to zero.

The algorithm for the time-dependent FE approach consists of the following two steps: First, determine a_{τ^1} by interpolating f_0 at interior knots and by imposing the boundary conditions in (19). Secondly, determine $a_\tau \in \Theta \backslash a_{\tau^1}$ recursively based on the following linear equation system:

$$(20) \qquad \underbrace{\begin{bmatrix} B_{I\cdot m}(\underline{m}) \\ \vdots \\ B(\underline{m}) \\ \mathbb{A}(\tau) \\ B(\overline{m}) \\ \vdots \\ B_{I\cdot m}(\overline{m}) \end{bmatrix}}_{N+K-1\times N+K-1} \begin{bmatrix} a_\tau^1 \\ a_\tau^2 \\ \vdots \\ a_\tau^{N+K-1} \end{bmatrix} = \underbrace{\begin{bmatrix} \hat{f}_{I\cdot m}(\underline{m}) \\ \vdots \\ \hat{f}(m^1) \\ \mathbb{C}(\tau)a_{\tau'} \\ \hat{f}(\overline{m}) \\ \vdots \\ \hat{f}_{I\cdot m}(\underline{m}) \end{bmatrix}}_{N+K-1\times 1}$$

The approximation in the first step could be substituted with the closed form expressions for f_0 and its derivatives.

It is worth noting that the linear equation system is banded with bandwidth $K-1$. This implies that a_τ can be determined with an operation count of $\mathcal{O}(N)$. I.e. the computational burden grows linearly with the number of B-splines in the basis. Especially, the equation system caused by a cubic spline approximation is tridiagonal as the corresponding equation system of popular FD methods like the Crank-Nicholson method.

3.4. BENCHMARK SETTINGS

The rest of the section examines the precision of the time-dependent FE approach for various orders and numbers of B-splines when applied to vanilla- and binary calls in the Black-Scholes setup. The parameter values used are $\sigma = 0.25$, $r = 0.03$, and $x = 100$. Maturities up to six months are considered. A number of settings are considered but they are all variations over the following benchmark settings: The knots M are equally spaced; the number of knots will vary. The artificial boundaries are chosen as $\underline{m} = -5.56$ and $\overline{m} = 8.70$ corresponding to $S(\underline{m}) = 0$ and $S(\overline{m}) = 2.5x$ respectively for $\tau = 0.5$. The time-transformed version of the PDE in (15) is used. Θ consists of 2500 time points equally spaced between $\theta^1 = 0$ and $\theta^{2500} = \sqrt{0.5}$, corresponding to $\tau \in [0, 0.5]$. Values of f for maturities not in Θ are found by linear interpolation. The Crank-Nicolson weight, $\omega = 1/2$, is used throughout.

The size of the approximation errors was calculated in two ways; in the supnorm and as a weighted average, each based on 300×300 equally spaced points $(m_\theta, \theta) \in [\underline{m},\ \overline{m}] \times [\sqrt{\text{1e-10}},\ \sqrt{0.5}]$.[7] A value of $\theta = \sqrt{\text{1e-10}}$ corresponds to approximately 0.001 seconds before maturity. The errors were calculated with respect to the closed form Black-Scholes option prices. The supnorm error is the highest absolute error value found. For calculating the weighted average approximation error, the absolute price errors were weighted in order to reflect the fact that at-the-money options are more important than out-of-the-money options. The weighting function use was the fundamental solution to the relevant heat equation in (5). I.e., all maturities were weighted equally.

The solutions are compared with traditional FD and FE approximations on a S_τ-space. The artificial boundaries in these cases were $\underline{S} = 0$ and $\overline{S} = 2.5x$, i.e., the stock prices corresponding to $\underline{m}$ and $\overline{m}$ for the longest maturity investigated. The traditional approximations are calculated for a non-transformed τ-based time space. For the FD approximation linear interpolation was used to evaluate points outside the approximation points.

Since the approximations of all methods in the section can be calculated for each maturity with an operation count of $\mathcal{O}(N)$, the methods are compared on the basis of the number of free parameters. For the m-based methods, the number of free parameters is the number of elements in a_τ.

For splines, a polynomial rate of convergence should be expected as the number of free parameters grows. More formally, $\|\epsilon_N\| = \mathcal{O}(N^{-\lambda})$ asymptotically, where ϵ_N is the error size subject to the relevant norm based on a number of N free parameters and λ is the

[7] The three points in the m dimension closest to x were moved closer to x in order to improve the calculation of the $supnorm$ error for the binary call.

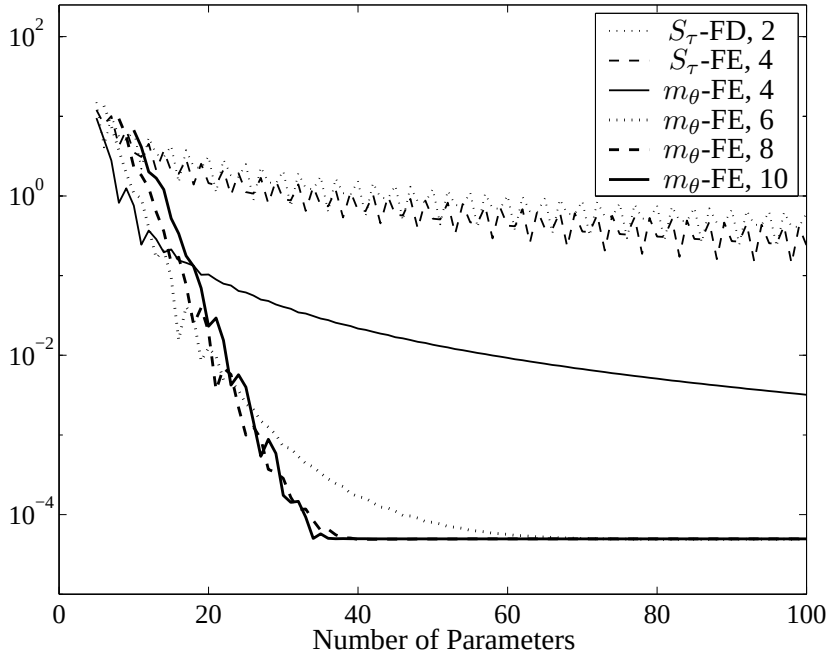

FIGURE 4: Supnorm errors for the vanilla call

polynomial rate of convergence estimated as

$$\lambda_{n,n-i} = -\frac{\log(\|\epsilon_n\|) - \log(\|\epsilon_{n-i}\|)}{\log(n) - \log(n-i)} \tag{21}$$

for a change of the number of free parameters from $n - i$ to n. The analysis follows Tavella and Randall (2000) and reports convergence rates for one dimension at a time. I.e., when convergence rates are calculated for approximations in the asset price dimension, the approximation precision of the time dimension is held fixed. The advantage is that the focus is on one approximation methods at the time. A drawback is that convergence rates can only be measured up to the precision of the approximation in the other dimension.[8] Below, the convergence rates are measured from $n - i = 5$ (or from where the approximation is defined) up to a number of parameters equal to $n = 100$, unless the approximation converged the lower bound of the time-dimension approximation with fewer than 100 parameters.

3.5. RESULTS ON SUPNORM ERRORS

Figure 4 reports the supnorm error for a number of vanilla call approximations on a logarithmic scale as functions of the number of free parameters.

First, compare the standard Crank-Nicolson FD solution, "S_τ-FD, 2", with a cubic spline FE approximation, "S_τ-FE, 4", applied on the (S_τ, τ)-space without transforma-

[8]For this reason, the number of points in the time dimension is chosen to be relatively high, 2500, for the benchmark setting.

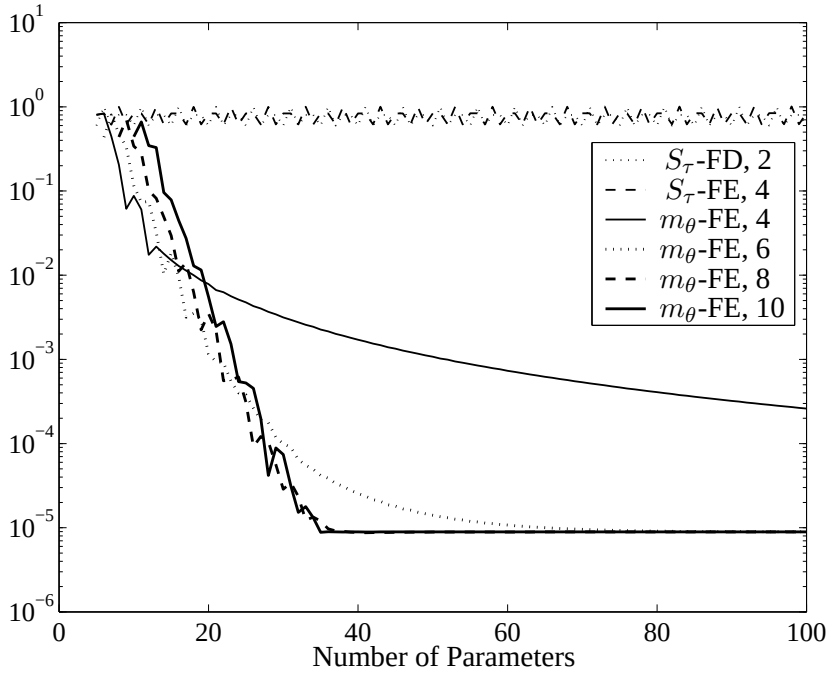

FIGURE 5: Supnorm errors for the binary call

tions. The Figure shows that although the cubic spline consistently has a higher precision, the difference between the two solutions is not significant. At first sight, also the convergence rates appear the same. The reason for this result is that the singularity point of the exact price function destroys the higher-order convergence properties of the cubic spline.

Turning to the approximations on the moneyness- and time-transformed state spaces (m_θ, θ), notice that the cubic spline approximation, labeled "m_θ-FE, 4", significantly outperforms the (S_τ, τ)-based cubic spline. Both in terms of level and order of convergence. However, splines of higher order, $K \in \{6, 8, 10\}$, appear even more powerful. The convergence rate for $K \in \{8, 10\}$ appear almost exponential before the approximation precision hits the lower bound precision of 5.0e-5 implied by the time dimension approximation precision.

The effect of the transformations are even more significant for the results on the binary call in Figure 5. The figure shows that the two approximations on the (S_τ, τ)-space does not even converge in the supnorm. The reason is, of course, that in the S_τ-space the payoff of the binary call jumps from zero to one close to maturity, and any continuous solution will have a supnorm error above 0.5. In the m_θ- space, however, the singularity is absent and the errors reported corresponds qualitatively to those of Figure 4.

Table 1 shows the polynomial rate of convergence as defined in (21) for supnorm errors. The listed methods correspond to the methods used in Figure 4 and 5. The "limit error" in the final column is an estimate of the highest possible precision without increasing the precision of the time-dimension approximation. The limit error is calculated as the lowest error obtained by the $K = 10$ approximation. I.e., the limit error of the default settings used by Figure 4 is 5.0e-5.

The table reports convergence rates for the benchmark settings as well as other settings. The "$\Theta \sim 250$" and "$\Theta \sim 25$" settings differ from the benchmark in that 250 and 25 approximation points were used for the time-dimension approximation instead of 2500 points. The "Time $\sim \tau$"- setting reports results for the τ-based PDE in (14) where the time transformation to θ has not been used. Finally, the results of "optimal" location of the spline knots are shown under "New Knots". The arguments for searching a better location of knots than the equally spaced knots are as follows. From Figure 2(a) it is seen that the solution to the problem is linear for most parts of the state space except for a small area around x, where the curvature of the solution is found. Based on this observation a conjecture might be that concentrating the spline knots, and thereby the flexibility, in the area of high curvature would increase precision. This idea is well-known, e.g. Tavella and Randall (2000), but the moneyness-transformed state space is particular suited for techniques improving the location of knots. Figure 2(a) shows that (unlike for the untransformed price function) the location of the curvature does not change much over time. Hence, there is little need to change the location of the optimal knots (and, hence, the approximation basis) as the solution algorithm works backwards in time. Moreover, the initial condition based on the limiting heat equation solution provides a fine a priori guess on where the curvature is located. As a result, there is no need to solve the problem first for, say, equally spaced knots in order to locate the area with high curvature. For the results in Table 1, the "optimal" location of knots were based on the NEWNOT algorithm as described in de Boor (1978) applied to the spline approximation of f_0.[9]

Consider first the results for the vanilla call in the first panel of Table 1. As expected, the traditional Crank-Nicolson method converges at a rate approximately linear in the supnorm which is the asymptotic convergence rate of linear methods applied to functions with kinks. With convergence rates between 1.04 and 1.43 the convergence rate of the traditional cubic spline is only slightly better than linear.[10]

The convergence rates of the four m-based approximations are, as expected from Figure 4, significantly higher than the rates of the S-based approximations. With a convergence rate of 2.67 for the benchmark setting, the cubic spline approximation, $K = 4$, the rate is twice the rate of the cubic spline approximation on the (S_τ, τ)-space. Still, the rate is lower than 4 which might be expected for well-behaved functions, e.g. de Boor (1978), but since the function is defined in terms of approximations of the functions own derivatives via the PDE, slower convergence of the derivative approximation might slow down the level-approximation also. The convergence rate is improved considerably by increasing the order of approximation beyond cubic. For the benchmark case, the rate for the six-order approximation, 5.45, is approximately twice the rate of the cubic approximation. The convergence rates for $K = 8$ and $K = 10$ are impressive, but should be interpreted with care as the range over which the rates are calculated is rather short, due to the fast convergence.

The time-dimension precision, $\Theta \sim 250$ and $\Theta \sim 25$, does not affect the convergence rate of the transformation method significantly. For $K = 10$ the rate seems to decrease with the precision, but since the convergence to the limit error level is almost immediately when the time-dimension precision is low, this estimate is uncertain.

[9] An implementation of NEWNOT is included in the commercial Matlab spline-toolbox.

[10] For the low precision setting, $\Theta \sim 25$, the traditional cubic spline diverged from some point. This explains the lower convergence rate in this case.

TABLE 1

CONVERGENCE RATES λ OF SUPNORM ERRORS

	S_τ-FD	S_τ-FE	m_θ-FE				Limit
	"$K = 2$"	$K = 4$	$K = 4$	$K = 6$	$K = 8$	$K = 10$	error
			Vanilla Call				
Benchmark	1.07	1.31	2.67	5.45	7.86	9.65	5.0e-5
$\Theta \sim 250$	1.07	1.43	2.68	5.51	7.76	8.63	5.0e-4
$\Theta \sim 25$	1.07	1.04	2.71	5.46	7.66	7.46	5.1e-3
Time $\sim \tau$	-	-	2.67	5.36	7.97	9.75	1.9e-5
New Knots	-	-	2.95	5.70	9.19	10.16	5.0e-5
			Binary Call				
Benchmark	0.00	-0.02	2.68	4.82	7.40	8.51	8.8e-6
$\Theta \sim 250$	0.00	-0.02	2.57	4.79	6.56	8.08	8.9e-5
$\Theta \sim 25$	0.00	0.02	2.32	4.46	5.84	6.69	9.1e-4
Time $\sim \tau$	-	-	2.49	4.79	6.55	7.70	1.8e-4
New Knots	-	-	2.75	4.91	8.00	9.03	8.9e-6

The limit errors of the first three lines clearly show that the non-central time-derivative approximation provides only first order convergence.

Since the convergence rates for the setting without time transformation, "Time $\sim \tau$", are similar to the rates of the benchmark case, the time transformation does not seem important for the vanilla case. The effect of the knot improvement method seems beneficial with an average improvement of the four convergence rates equal to 0.6.

Consider next the results for the binary call in the second panel of Table 1. As expected from Figure 5, the traditional S-based methods show no sign of convergence in the supnorm. For the m-based approximations, all convergence rates are lower than for the vanilla case, with one minor exception.

Unlike the vanilla case the rates for the binary payoff seem to be affected positively by the time-transformation. The τ based convergence rates are on average 0.56 lower than the benchmark rates. The estimated rates should be interpreted with care since the limit error is raised significantly compared to the benchmark settings. As a result, especially the high order methods $K \in \{8, 10\}$ must be estimated over a very short interval.

Finally, the effect of the knot improvement method is, with an average of 0.4, a bit lower than in the vanilla case.

3.6. AVERAGE ERRORS RESULTS

The supnorm error measures the largest pricing error of the state space. Despite the intuitive appeal, the supnorm might give the wrong impression if the general precision

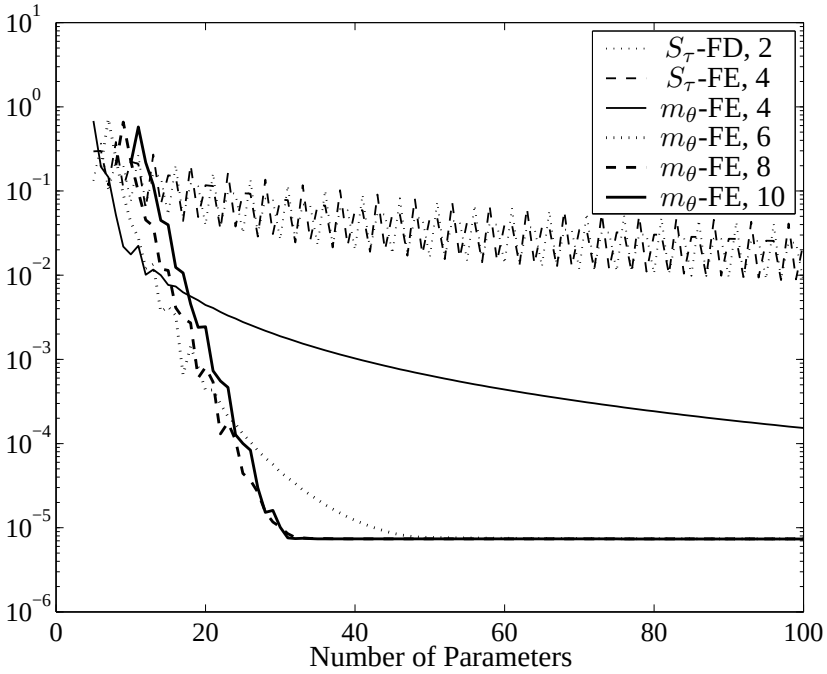

FIGURE 6: Weighted average errors for the binary call

over the entire state space is of interest. This might well happen in the option pricing case where the price approximation is likely to be poor around a singularity point and much better on the rest of the state space. To investigate this conjecture the weighted average errors are analyzed.

Figure 6 corresponds to Figure 5 except that errors are measured as weighted average instead of supnorm errors for the binary call approximation. Contrary to the supnorm errors, the average errors show a clear convergence for the two S-based methods. Still, there seems to be only a little precision gain from using the cubic spline instead of the FD method. With respect to the m-based methods, there seems to be only small changes relative to the supnorm error results. Convergence rates of average errors are reported in Table 2 which is otherwise identical to Table 1.

Turning to the vanilla call panel first, the table shows a significant improvement in convergence speed for the S-based methods compared with the supnorm figures. Since the Crank-Nicolson method attain a quadratic convergence rate, which is the highest possible, it is concluded that the singularity has little influence on the general precision of the approximation for the number of parameters investigated. Unlike the Crank-Nicolson approximation, but in line with the m-based cubic spline, the S-based cubic spline is far from reaching the convergence rate potential of 4 for smooth functions. However, as for the supnorm errors, the cubic spline approximation converges a bit faster than Crank-Nicolson for the default settings. With the exception of the cubic spline, the m-based approximations show higher convergence rates than for the supnorm errors in Table 1. With an average convergence order increase for the benchmark at 0.76, $K \in \{4, 6, 8, 10\}$, the change is almost as significant as the increase of order for the S-based methods.

TABLE 2

CONVERGENCE RATES OF AVERAGE ERRORS

	S_τ-FD	S_τ-FE	m_θ-FE				Limit
	"K = 2"	K = 4	K = 4	K = 6	K = 8	K = 10	error
	Vanilla Call						
Benchmark	2.02	2.36	2.40	6.24	9.19	10.82	2.1e-5
$\Theta \sim 250$	2.02	2.28	2.41	6.52	9.03	9.94	2.0e-4
$\Theta \sim 25$	2.04	1.40	2.39	6.55	8.09	8.79	2.0e-3
Time $\sim \tau$	-	-	2.40	6.08	9.20	10.62	1.2e-5
New Knots	-	-	2.94	8.07	10.95	11.73	2.1e-5
	Binary Call						
Benchmark	0.92	0.83	2.80	5.06	7.49	9.06	7.4e-6
$\Theta \sim 250$	0.92	0.83	2.73	4.99	6.87	8.27	7.4e-5
$\Theta \sim 25$	0.90	0.80	2.81	5.08	6.19	7.16	7.1e-4
Time $\sim \tau$	-	-	2.70	5.16	7.45	9.09	1.3e-5
New Knots	-	-	3.36	6.77	8.81	10.27	7.2e-6

As for the supnorm errors, the θ transformation does not seem to matter a lot whereas the improved knot placement increases the convergence rates for the vanilla call significantly. The average effect is 1.26 compared to the benchmark results.

Next, consider the binary panel. According to Figure 6, the Crank-Nicolson approximation is expected to converge. If the effect of the singularity is restricted to a small area, the convergence might be quadratic as in the vanilla case. Table 2 shows that the convergence rate is hardly linear. The effect of the singularity is even more significant for the S-based cubic spline which converges slower than the Crank-Nicolson approximation. For both Crank-Nicholson and the cubic spline, the relative improvement compared to the supnorm case is, however, somewhat similar to the relative improvement in the vanilla case. As expected, the convergence rate of the m-based approximations are with no exceptions higher for the average errors compared to the supnorm error in Table 1.

Note finally, that the limit error for all settings are of the same magnitude for supnorms and averages, perhaps with the τ-based binary call approximations as the only exception. This result suggests that the 10'th order approximations, with which the limit error is calculated, are of the same quality over the entire state space.

3.7. PRECISION OF THE GREEKS

An issue of great practical importance for hedging is the derivatives of the option price with respect to the underlying asset price. Table 3 shows convergence rates and limit errors for first- and second-order derivatives (known as *delta* and *gamma*) for the benchmark

TABLE 3

CONVERGENCE RATES OF DERIVATIVE ERRORS

		S_τ-FD	S_τ-FE	m_θ-FE				Limit
		"K = 2"	K = 4	K = 4	K = 6	K = 8	K = 10	error
		1. Order Derivative (Delta)						
Sup	Vanilla	0.00	-0.00	2.31	4.77	6.76	7.87	4.7e-4%
	Binary	0.00	0.00	3.00	5.20	7.66	9.83	5.8e-5%
Avr	Vanilla	1.22	1.46	2.32	5.09	7.52	8.86	4.9e-4%
	Binary	0.00	0.00	3.02	5.55	8.14	10.25	5.5e-5%
		2. Order Derivative (Gamma)						
Sup	Vanilla	0.00	0.00	2.01	4.54	6.99	9.26	6.2e-5%
	Binary	-0.00	-0.00	1.99	4.17	6.62	8.65	5.1e-4%
Avr	Vanilla	0.00	0.00	2.33	4.64	7.27	9.60	6.0e-5%
	Binary	0.00	0.00	2.15	4.37	6.84	9.01	2.0e-4%

case. Both supnorm and average errors are shown, all for the benchmark setting. Note that the limit errors are reported in percentages. The supnorm limit errors are expressed as a percentages of the highest derivative value of the state space. Similarly the average limit errors are percentages of the average values over the state space. The reason for this normalization is that the size of some derivatives is quite big for the shortest maturities investigated (0.001 seconds).[11]

Starting with the first order derivatives (delta), Table 3 shows that the two S-based methods does not converge in the supnorm. This result is expected due to the jump in delta at the singularity. On average, the delta of the two methods converges for the vanilla payoff with relative high rates of 1.22 and 1.46. It is somewhat surprising that there is no sign of convergence for averages in the binary case.

Turning to the m-based results it would be natural to expect the convergence rate of delta to be one order lower than the price level. This conjecture is not supported by the results in Table 3 when compared with the benchmark results of the previous tables. For the vanilla payoff, the convergence rate of the level dominates the rate of the derivatives but for the binary payoff, the delta convergence rate dominates. The limit errors between 5.5e-5 and 4.8e-4 are small for practical purposes.

When turning to the second order derivatives (gamma) it comes as no surprise, given the results for delta, that the two S-based methods do not converge. The convergence rates of the m-based methods are in general of the same order as the rates of delta. There seems to be no clear picture in the individual differences. The gamma limit errors are of the same

[11] For the vanilla call the supremum of gamma over the state space is 1595.77 and the average 3.79. For the binary call the corresponding figures are 3.878e+6 and 8444.97.

magnitude as the delta limit errors.

4. Full Finite Element Approximations

One drawback of the time-dependent FE approach is the relative low precision of the approximation in the time dimension. The non-central derivative approximation converges with only a linear rate, as shown by the limit errors in Table 1 and 2. As a result, a relative high number of time-steps are needed. One alternative is to consider higher-order FE approximations in the time dimension if the function of interest is well behaved in the time dimension. Figure 2 suggests that this indeed the case for $f(m_\tau, \tau)$. This section investigates the properties of a full FE approximation generated by tensor splines.

4.1. The Approximation Basis

In order to define the two-dimensional tensor spline approximation basis, the basis already constructed for the m dimension in Section 3 will used together with a similar spline approximation basis in the time dimension. To define the latter, consider a series of knots in the time dimension, $\xi^j \in \Xi = [\xi^1, \xi^2, \dots \xi^{J+1}]$. If properly augmented with multiplicity K^τ at the endpoints, where K^τ is the spline order of the time dimension approximation, these knots define the wanted basis over J subintervals on the interval $\tau \in [\underline{\tau}, \overline{\tau}] = [\xi^1, \xi^{J+1}]$, with the number of B-splines equal to $J + K^\tau - 1$. Let $B^j(\tau),\ j \in \{1, 2, \dots, J + K^\tau - 1\}$ denote the values of the individual B-splines at τ, and let them be ordered in the vector $B(\tau) = [B^1(\tau)\ \ B^2(\tau)\ \ \dots\ B^{J+K^\tau-1}(\tau)]$. Now, the individual tensor B-splines are defined as

$$B^{n,j}(m_\tau, \tau) = B^n(m_\tau)B^j(\tau), \qquad \begin{array}{l} n \in \{1, 2, \dots, N + K - 1\} \\ j \in \{1, 2, \dots, J + K^\tau - 1\} \end{array}$$

where $B^n(m_\tau)$ is defined in Section 3. To ease the notation, the total number of B-splines equal to $(N + K - 1) \times (J + K^\tau - 1)$ are ordered in the vector

$$B(m_\tau, \tau) = B(m_\tau) \otimes B(\tau) \tag{22}$$

where $B(m_\tau)$ is defined in Section 3. Finally, the full approximation is defined as a linear function of the individual tensor B-splines,

$$f(m_\tau, \tau) \approx B(m_\tau, \tau, \gamma) = B(m_\tau, \tau)\gamma, \tag{23}$$

where γ is the vector of free parameters to be determined. Since the approximation in (23) is continuous in time, the time-derivative $B_\tau(m, \tau)$ is obtained simply by substituting $B(\tau)$ in (22) with values of $B_\tau(\tau) = \partial B(\tau)/\partial\tau$. The derivatives in the m-dimension, $B_m(m_\tau)$, $B_{mm}(m_\tau)$, etc. are obtained similarly. Note that since the approximation is continuous in time, a natural distinction between explicit, implicit, and Crank-Nicolson methods disappear.

With properly defined coefficients, β, the restrictions imposed by the relevant PDE for a single point (m_τ, τ) takes the following compact form:

$$\big(\beta_0 B(m_\tau,\tau)+\beta_1 B_\tau(m_\tau,\tau)-\beta_2 B_m(m_\tau,\tau)-\beta_3 B_{mm}(m_\tau,\tau)\big)\gamma_\tau=0$$

(24) $$\Downarrow$$

$$A(m_\tau,\tau)\gamma=0.$$

As indicated, the restriction is linear in γ. In order to determine the coefficients, a number of approximation points must be chosen. For the m dimension, the approach of Section 3 is adapted here: Interpolation at interior spline knots and boundary conditions on the level and a varying number of derivatives. For the time dimension, boundary conditions are not available and instead the number interpolation points are increased accordingly. Hence, define the series of approximation points $\Theta=[\tau^1,\tau^2,\ldots,\tau^{J+K^\tau-1}]$, with $\tau^1=\underline{\tau}$ and $\tau^{J+K^\tau-1}=\overline{\tau}$. As a result of the "extra" points, the interpolation restrictions will not coincide with the spline knots in general.

The interpolation restriction in (24) will be imposed on all interior approximation points as well as for the end-points at $\tau=\overline{\tau}$. Note first that since the approximation basis can be decomposed into a m_τ-dependent and a τ-dependent part, the same is possible for the interpolation condition,

(25) $$\Big(A(m_\tau)\otimes A(\tau)\Big)\gamma=0.$$

Define then the following temporary matrices according to the decomposition in (25),

$$\mathbb{A}(m_\tau)=\begin{bmatrix}A(m^2)\\ \vdots\\ A(m^N)\end{bmatrix},\quad\text{and}\quad \mathbb{A}(\tau)=\begin{bmatrix}A(\tau^2)\\ \vdots\\ A(\tau^{J+K^\tau-1})\end{bmatrix},$$

in order to define all interpolation conditions as the following linear equation system:

(26) $$\mathbb{A}\gamma=0,\qquad\text{where}\qquad \mathbb{A}=\mathbb{A}(m_\tau)\otimes\mathbb{A}(\tau)$$

The system in (26) provide $(N-1)\times(J+K^\tau-2)$ conditions of a total of $(N+K-1)\times(J+K^\tau-1)$ needed. From interpolation conditions with respect to the initial condition, $N-1$ linear restrictions are added:

(27) $$B(m^n,0)\gamma=f_0(m^n),\qquad n=2,\ldots N.$$

The remaining $K\times(J+K^\tau-1)$ restrictions are provided by the boundary conditions at $\underline{m}$ and $\overline{m}$,

(28) $$\begin{aligned}B_{i\cdot m}(\underline{m},\tau^j)\gamma&=\hat{f}_{i\cdot m}(\underline{m},\tau^j),\\ B_{i\cdot m}(\overline{m},\tau^j)\gamma&=\hat{f}_{i\cdot m}(\overline{m},\tau^j)\end{aligned}\quad,\quad j=1,\ldots,J+K^\tau-1,\;\; i=0,\ldots,\frac{K}{2}-1,$$

where $B_{0\cdot m}(m_\tau,\tau)$ and $f_{0\cdot m}(m_\tau,\tau)$ denote the levels.

COMPUTATIONAL ASPECTS

The linear equation system (26), (27), and (28) is not banded as the system in (20). Due to the finite element basis, the system will be sparse, however. Although the system display a fairly regular sparsity pattern, this patterns is not particularly desirable from a computational point of view, e.g. Rust (1994), and general approaches for dealing with sparse problems must be applied if the sparsity is to be used to speed up the calculations.[12]

Although the structure of the full FE system is less attractive than the time-dependent version, the former has an important advantage. The time-dependent system required an operation count of $\mathcal{O}(N \times J)$ to determine the approximation but J had to be large (2500 as default). Below it is shown that J can be reduced from 2500 in the time-dependent FE case to 5 in the full FE case without losing precision.

BENCHMARK SETTINGS

The benchmark setup is basically the same as for the time-dependent FE approach. With respect to the time-dimension approximation, the θ-based PDE is used. An implementation based on the τ-based PDE was tried but due to instability for high-precision solutions, a thorough investigation was not conducted. As before, maturities of up to six months are considered. Both the spline knots and the approximation points are equally spaced.

4.2. RESULTS

To investigate convergence rates of various orders for spline approximations of the time dimension, the m dimension approximation was fixed at a high quality 10'th order spline with 40 free parameters. In Figure 7, the supnorm errors of vanilla call-approximations are shown for various orders and various numbers of free parameters in the time dimension. The figure shows that the FE-approach is very effective in this case. With only nine free parameters all spline orders, except the quadratic, have converged to the lower bound: The limit error implied by the high quality m dimension approximation. In fact, the convergence is so fast that for most orders the convergence rate cannot be determined. It is worth noting that the cubic spline ($K = 4$) over two subintervals (5 free parameters), provide a precision higher than the time-dependent FE solution of Section 3 with 2500 free parameters/time steps.

Figure 8 returns to the question of convergence rates of approximations in the m dimension and investigate if the FE approximation affects the convergence rates of Section 3. The 2500 points used for the FD approximation in Section 3 are replaced by a 8'th order spline over three subintervals. I.e., a total number of free parameters equal to 10 in the time dimension. The Figure shows both supnorm errors and weighted average errors for vanilla call-approximations. Turning to the supnorm errors in Figure 8(a) first, the most remarkable difference to the comparable Figure 4 is that the limit error has decreased significantly from 5.0e-5 (benchmark) for the time-dependent FE approximation to 3.7e-7 for the full FE approximation.

Turning to the average errors, the fall in the limit error from 2e-5 in Table 2 (benchmark) to 4.3e-11 in Figure 8(b) is even more dramatic. Because of the very high precision,

[12] Algorithms for dealing with sparse problems are readily available in, for instance, Matlab.

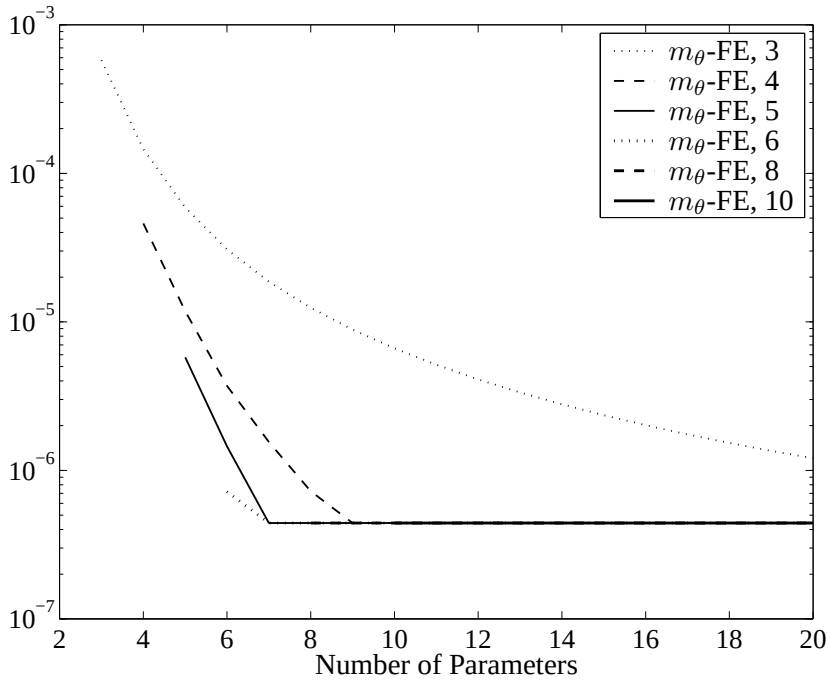

FIGURE 7: Supnorm errors for vanilla call

even the 10'th order spline barely reaches the limit error with 100 free parameters in the m dimension. It is worth noting that the total number of free parameters for the entire approximation equals the parameter numbers reported in Figure 4 multiplied with only 10. I.e., with 500 parameters it is possible to reach a level of precision approximately equal to 3e-7 in the supnorm and 1e-8 on average. Calculations show that the corresponding numbers for the binary call are approximately 1e-7 and 4e-9.

Table 4 reports the convergence rates and limit errors with the same time dimension approximation as used in Figure 8. Option price levels, first- and second-order derivatives (delta and gamma) are investigated in both supnorm and averages for vanilla and binary calls.

The results can be summarized roughly as follows. For the cubic spline approximation, both price level, delta, and gamma converges with a quadratic rate. The rate falls slightly from level to delta and from delta to gamma. The same comments apply for the other approximations except that the convergence rates are roughly $\lambda = 5$ for $K = 6$, $\lambda = 8$ for $K = 8$, and $\lambda = 10$ for $K = 10$. Compared with the results of the time-dependent FE approach in Section 3, this implies that for $K \in \{4, 6\}$, the convergence rates are similar. For $K \in \{8, 10\}$, the results reported in Table 4 dominates, with few exceptions, the corresponding figures in Section 3. Note, however, that the limit errors are significantly smaller in Table 4 than in Section 3 although the number of parameters used for the time dimension approximation is significantly lower. The size of the limit errors in Table 4 are small for most purposes.

TABLE 4

CONVERGENCE RATES OF FULL FE ERRORS

		m_θ-FE				Limit error
		K = 4	K = 6	K = 8	K = 10	
		Option Price				
Supnorm	Vanilla	2.66	5.46	8.58	10.78	3.7e-07
	Binary	2.62	4.99	7.95	9.91	1.2e-07
Average	Vanilla	2.41	5.66	8.51	11.52	4.3e-11
	Binary	2.69	4.96	7.73	10.89	2.5e-10
		1. Order Derivative (Delta)				
Supnorm	Vanilla	2.31	4.78	7.32	8.94	1.6e-05%
	Binary	2.46	4.99	7.87	9.59	1.5e-08%
Average	Vanilla	2.32	4.87	7.64	10.50	1.0e-09%
	Binary	2.07	4.65	7.38	10.19	4.4e-10%
		2. Order Derivative (Gamma)				
Supnorm	Vanilla	2.08	4.47	7.29	9.72	3.4e-08%
	Binary	1.93	4.22	6.67	8.86	3.1e-10%
Average	Vanilla	2.06	4.56	7.25	9.95	5.6e-11%
	Binary	2.00	4.34	6.98	9.55	9.4e-14%

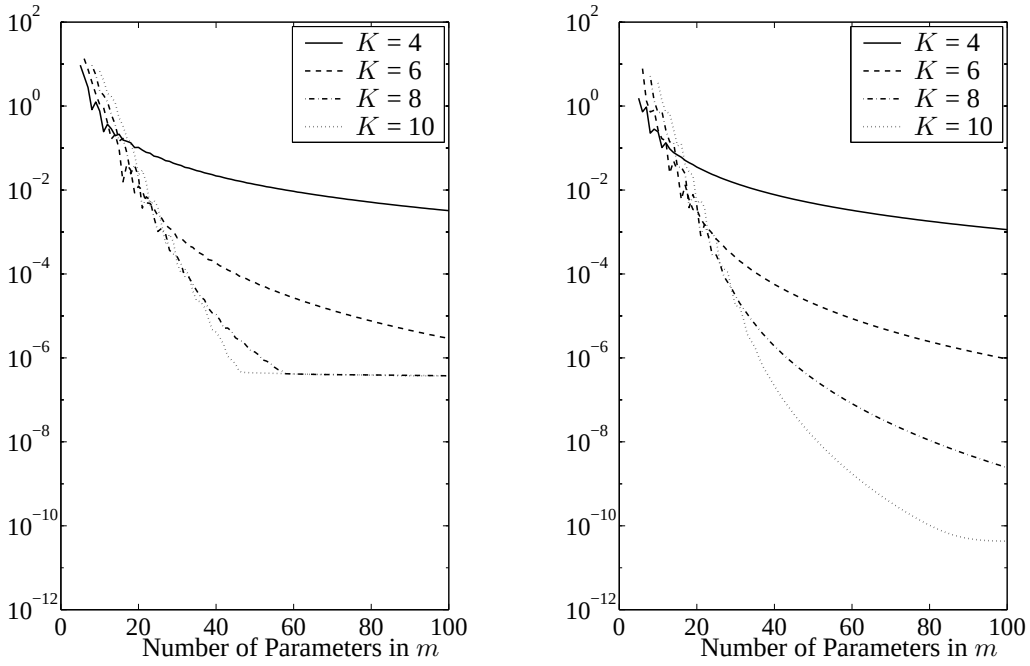

(a) Supnorm

(b) Weighted Average

FIGURE 8: Vanilla call errors

4.3. AN ALTERNATIVE REMEDY

One alternative to the approach suggested above is the grid positioning method suggested by Tavella and Randall (2000) and extended with "Rannacher time-stepping" by Pooley, Vetzal, and Forsyth (2003). The two studies find that neither the averaging methods nor the projection method performed significantly better than the grid positioning method. Figure 9 reports the results of the grid positioning method with the time-stepping suggested by Pooley, Vetzal, and Forsyth (2003) applied to the benchmark settings above. In addition to the usual two error measures, the numerical pricing errors of an at-the-money option with six months to maturity are reported; all as functions of the total number of free parameters used by the approximation.

Figure 9 show two important points. First, the efficiency of linear methods with respect to the number of free parameters used is low compared with the results in Figure 8. Despite the remedies, the Crank-Nicolson solution of the vanilla call which uses ten million parameter are dominated by the transformation method results with 40×10 free parameters. Both with respect to supnorm- and average errors. Calculations show that the differences are even more significant for the binary call.

Second, Figure 9(a) shows that the "single-point error" of the vanilla call is representative for the average error level. All error measures converge with approximately the same rate. However, from Figure 9(b) it is clear that this is not the case for the binary call. The supnorm error will not fall below 0.5 and the average error only converges with a high rate until a certain level of precision. This is not the case for the single-point error which keeps on converging at a steady rate. If average or supnorm precision is wanted, results based

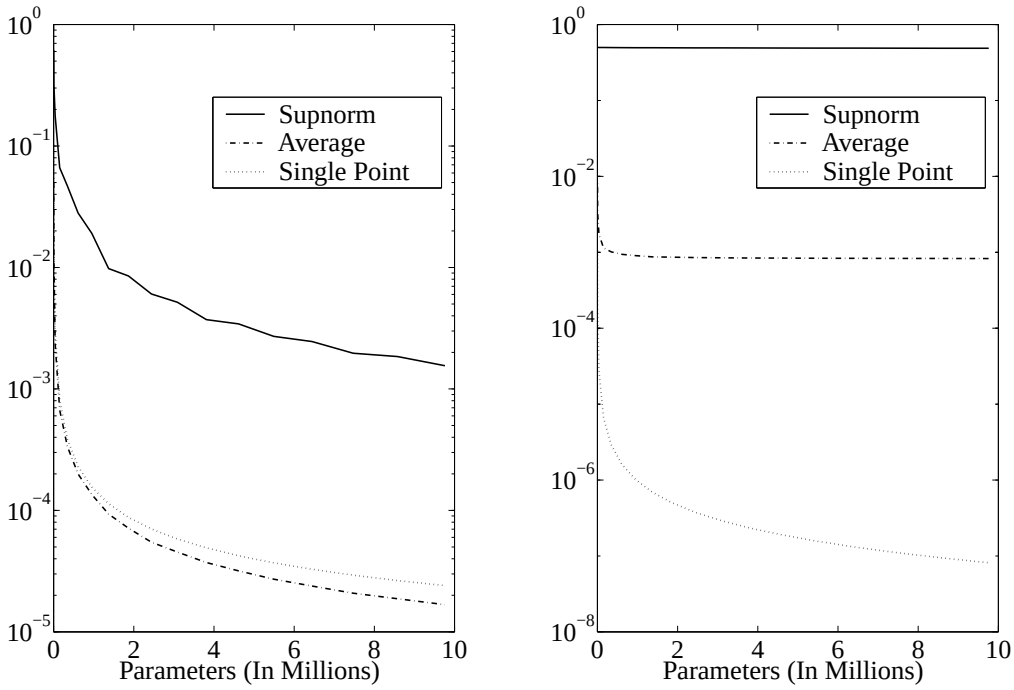

(a) Vanilla Call (b) Binary Call

FIGURE 9: Price level errors for the grid positioning method

Following Pooley, Vetzal, and Forsyth (2003) the figures are based on a traditional Crank-Nicolson solutions with the first two steps being implicit, (Rannacher time-stepping). Also the number of grid points in the time dimension is chosen to be approximately 61% of the number of points in the asset price dimension. The number of parameters refer to the total number of free parameters in the approximation including both time- and asset price dimensions. For the vanilla call, the gridpoints were chosen such that the a gridpoint is placed exactly at the exercise price, x. For the binary call, the gridpoints were chosen such that the exercise price were exactly in the middle of two points. The single point-errors refer to the pricing error of an at-the-money option with six months to maturity. Other settings are similar to the standard settings used for the rest of the paper.

on single-point errors should therefore be interpreted with care.

5. Conclusion

Due to payoff function singularities, higher-order numerical methods cannot be applied directly to option pricing problems successfully. This paper suggested a transformation method to turn the original ill-conditioned problem into a well-behaved numerical problem.

Applications to vanilla- and binary call options in the classical Black-Scholes setting showed that the transformation method worked successfully in this case. Convergence rates of orders of up to approximately 10 were observed for price level, delta, and gamma. The results were obtained in the supnorm and for averages as well as for a time-dependent FE method and for a pure FE method. As a result of the fast convergence, very small error levels were obtained for the entire state space with only few parameters to determine by a sparse linear equation system. High precision is attractive in connection with, for instance, empirical estimations were the calculation of the option price function is a problem nested in an estimation routine. High precision will help the optimization routine, and since empirical observations will be scattered, precision is wanted for the entire state space.

Only European type options on one-dimensional time-dependent state spaces were considered. If similar results can be obtained for options with American elements and multi-dimensional state spaces will be subject to future research.

Appendix A Convergence to the Heat Equation

The relevant PDE for the option pricing function is given as:

$$r(S_t,t)U(S_t,t) = \frac{\partial U}{\partial t} + r(S_t,t)S_t\frac{\partial U}{\partial S} + \tfrac{1}{2}\sigma(S_t,t)^2\frac{\partial^2 U}{\partial S^2}. \tag{29}$$

Consider now the transformations:

$$\tau = T - t, \qquad s_\tau = S_t e^{r_0\tau}, \qquad \text{and} \qquad u(s_\tau,\tau) = U(S_t,t)\; e^{r_0\tau}$$

where $r_0 = r(x,0)$. Then,

$$\begin{aligned}
\frac{\partial U}{\partial \tau} &= -\frac{\partial}{\partial \tau}u(s_\tau,\tau)\; e^{-r_0\tau} \\
&= \left(\frac{\partial u}{\partial \tau} + \frac{\partial u}{\partial s}\frac{\partial s}{\partial \tau} - r_0 u\right) e^{-r_0\tau} \\
&= \left(\frac{\partial u}{\partial \tau} + r_0 s\frac{\partial u}{\partial s} - r_0 u\right) e^{-r_0\tau}, \quad \text{since} \quad \frac{\partial s}{\partial \tau} = r_0 S_t e^{r_0\tau} = r_0 s_\tau,
\end{aligned}$$

$$\frac{\partial U}{\partial S} = \frac{\partial}{\partial S} u(s_\tau, \tau)\, e^{-r_0 \tau}$$

$$= \frac{\partial u}{\partial s}\frac{\partial s}{\partial S} e^{-r_0\tau}$$
$$= \frac{\partial u}{\partial s}, \qquad \text{since} \qquad \frac{\partial s}{\partial S} = e^{r_0\tau},$$

$$\frac{\partial^2 U}{\partial S^2} = \frac{\partial^2 u}{\partial s^2}\frac{\partial s}{\partial S}$$
$$= \frac{\partial^2 u}{\partial s^2} e^{r_0\tau}.$$

Inserting in (29) and rearranging gives

$$(r(s_\tau,\tau) - r_0)u = -\frac{\partial u}{\partial \tau} + (r(s_\tau,\tau) - r_0)s_\tau \frac{\partial u}{\partial s} + \tfrac{1}{2}\sigma(s_\tau,\tau)^2 \frac{\partial^2 u}{\partial s^2} e^{2r_0\tau}.$$

Letting $(s_\tau, \tau) \to (x, 0)$ gives $r(s_\tau, \tau) \to r_0$ and $\sigma(s_\tau, \tau) \to \sigma_0$, where $\sigma_0 = \sigma(x, 0)$. As a result,

$$\frac{\partial u}{\partial \tau} = \tfrac{1}{2}\sigma_0^2 \frac{\partial^2 u}{\partial s^2}.$$

Moreover, since $s_t \to S_t$ and $u \to U$ for $\tau \to 0$,

$$\frac{\partial U}{\partial \tau} = \tfrac{1}{2}\sigma_0^2 \frac{\partial^2 U}{\partial S^2}.$$

APPENDIX B HEAT EQUATION WITH VANILLA CALL INITIAL CONDITION

The payoff function $u(s, 0) = \max(s - x, 0)$ is inserted in (9) gives:

$$\begin{aligned}
u(s_\tau,\tau) &= \frac{1}{\sqrt{2\pi\tau\sigma_0^2}} \int_{-\infty}^{\infty} u(s,0) e^{-\frac{1}{2}\left(\frac{s-s_\tau}{\sqrt{\tau}\sigma_0}\right)^2} ds \\
&= \frac{1}{\sqrt{2\pi}} \int_{-\infty}^{\infty} u\left(y\sigma_0\sqrt{\tau} + s_\tau, 0\right) e^{-\frac{1}{2}y^2} dy \\
&= \frac{1}{\sqrt{2\pi}} \int_{-\frac{s_\tau - x}{\sigma_0\sqrt{\tau}}}^{\infty} (y\sigma_0\sqrt{\tau} + s_\tau - x) e^{-\frac{1}{2}y^2} dy \\
&= (s_\tau - x)\Phi\left(\frac{s_\tau - x}{\sigma_0\sqrt{\tau}}\right) + \sigma_0\sqrt{t}\ \phi\left(\frac{s_\tau - x}{\sigma_0\sqrt{\tau}}\right) \\
&= \sqrt{\tau}\ \sigma_0 \left(m_\tau \Phi(m_\tau) + \phi(m_\tau)\right), \qquad m_\tau = \frac{s_\tau - x}{\sigma_0\sqrt{\tau}}
\end{aligned} \tag{30}$$

which suggests $g(\tau) = \sqrt{\tau}$.

APPENDIX C HEAT EQUATION WITH BINARY CALL INITIAL CONDITION

The payoff function $u(s,0) = \mathcal{H}(s-x)$ is inserted in (9) gives:

$$
\begin{aligned}
u(s_\tau,\tau) &= \frac{1}{\sqrt{2\pi\tau\sigma_0^2}} \int_{-\infty}^{\infty} u(s,0) e^{-\frac{1}{2}\left(\frac{s-s_\tau}{\sqrt{\tau}\sigma_0}\right)^2} ds \\
&= \frac{1}{\sqrt{2\pi}} \int_{-\infty}^{\infty} u\left(y\sigma_0\sqrt{\tau}+s_\tau,0\right) e^{-\frac{1}{2}y^2} dy \\
&= \frac{1}{\sqrt{2\pi}} \int_{-\frac{s_\tau-x}{\sigma_0\sqrt{\tau}}}^{\infty} e^{-\frac{1}{2}y^2} dy \qquad (31) \\
&= \Phi\left(\frac{s_\tau-x}{\sigma_0\sqrt{\tau}}\right) \\
&= \Phi(m_\tau), \qquad m_\tau = \frac{s_\tau-x}{\sigma_0\sqrt{\tau}}
\end{aligned}
$$

which suggests $g(\tau) = 1$.

APPENDIX D PROPERTIES OF FIXED BOUNDARIES IN THE M-SPACE

When artificial boundaries are introduced, a fraction of the effect caused by the singularity in the payoff function are truncated. This appendix shows that for solutions to the limiting heat equation this fraction is constant over time for constant bounds in the m-space.

D.1 THE FUNDAMENTAL SOLUTION

Let $G(S_\tau,\tau)$ be the fundamental solution from (5). The cumulative effect up to $S_\tau = a$ at τ is defined as

$$
E(\widetilde{s},\tau) = \int_{-\infty}^{\widetilde{s}} |G(s,\tau) - G(s,0)| ds
$$

Changing measure from s to m gives

$$
E(\widetilde{m},\tau) = \int_{-\infty}^{\widetilde{m}} |\phi(m) - \delta(m)| dm
$$

where $\widetilde{m} = (\widetilde{s}-x)/(\sigma\sqrt{\tau})$ and the change of measure w.r.t. the Dirac-function is a bit delicate. Note that $E(\infty,\tau) = 2$.

It is easily seen that the cumulative effect is time- independent. Hence, by determining the lower artificial boundary $\underline{m}$ according to

$$
\frac{E(\underline{m},\tau)}{E(\infty,\tau)} = \alpha, \qquad 0 < \alpha < 1,
$$

a fraction α of the total effect will be truncated and this fraction will be time-independent. The analysis for $\overline{m}$ is similar.

D.2 VANILLA CALL PAYOFF

Let $u(s_\tau, \tau)$ be given by equation (10). The cumulative effect of the payoff singularity is then

$$E(\widetilde{s}, \tau) = \int_{-\infty}^{\widetilde{s}} |u(s, \tau) - \max(s - x, 0)| ds$$

Change of measure to m gives

$$E(\widetilde{m}, \tau) = \tau\sigma^2 \int_{-\infty}^{\widetilde{m}} |m\Phi(m) + \phi(m) - \max(m, 0)| \, dm$$

Although $E(\widetilde{m}, \tau)$ is time-dependent, the ratio $E(m, \tau)/E(\infty, \tau)$ is not, since the τ-terms cancels out. And the wanted result follows.

D.3 BINARY CALL PAYOFF

For the binary call, the cumulative effect function in m is given by

$$E(\widetilde{m}, \tau) = \sqrt{\tau}\sigma \int_{-\infty}^{\widetilde{m}} |\Phi(m) - \mathcal{H}(m)| \, dm$$

Again, the effect is time-dependent, but ratios are not, as in the vanilla call case above.

APPENDIX E TRANSFORMED PDE

The relevant PDE for the option pricing function is given as:

$$r(S_t, t)U(S_t, t) = \frac{\partial U}{\partial t} + r(S_t, t)S_t \frac{\partial U}{\partial S} + \tfrac{1}{2}\sigma(S_t, t)^2 \frac{\partial^2 U}{\partial S^2}. \tag{32}$$

E.1 TRANSFORMED PDE, BASED ON τ

Consider now the transformations:

$$\begin{aligned}
\tau &= T - t, \\
s_\tau &= S_\tau e^{r_0 \tau}, \\
u(s_\tau, \tau) &= U(S_t, t) e^{r_0 \tau}, \\
m_\tau &= \frac{s_\tau - x}{\sigma_0 \sqrt{\tau}}, \\
g(\tau) f(m_\tau, \tau) &= u(s_\tau, \tau),
\end{aligned}$$

where $r_0 = r(x, 0)$ and $g(\tau)$ is known. Then

$$\begin{aligned}
\frac{\partial U}{\partial t} &= -\frac{\partial}{\partial \tau} g(\tau) f(m_\tau, \tau) e^{-r_0 \tau} \\
&= -g(\tau) \left(\frac{\partial g / \partial \tau}{g(\tau)} f + \frac{\partial f}{\partial \tau} + \frac{\partial f}{\partial m} \frac{\partial m}{\partial \tau} - r_0 f \right) e^{-r_0 \tau}
\end{aligned}$$

and

$$\begin{aligned}\frac{\partial U}{\partial S} &= g(\tau)\frac{\partial f}{\partial m}\frac{\partial m}{\partial s}\frac{\partial s}{\partial S}e^{-r_0\tau} \\ &= g(\tau)\frac{\partial f}{\partial m}\frac{\partial m}{\partial s}\end{aligned}$$

and

$$\begin{aligned}\frac{\partial^2 U}{\partial S^2} &= g(\tau)\frac{\partial^2 f}{\partial m^2}\left(\frac{\partial m}{\partial s}\right)^2\frac{\partial s}{\partial S} + g(\tau)\frac{\partial f}{\partial m}\frac{\partial^2 m}{\partial s^2}\frac{\partial s}{\partial S} \\ &= g(\tau)\left(\frac{\partial^2 f}{\partial m^2}\left(\frac{\partial m}{\partial s}\right)^2 + \frac{\partial f}{\partial m}\frac{\partial^2 m}{\partial s^2}\right)e^{r_0\tau}.\end{aligned}$$

Collecting everything and inserting in (32) leads to

$$\begin{aligned}&\left(r_\tau - r_0 + \frac{\partial g/\partial\tau}{g(\tau)}\right)f \\ &= -\frac{\partial f}{\partial\tau} + \left(r_\tau s_\tau\frac{\partial m}{\partial s} - \frac{\partial m}{\partial\tau} + \tfrac{1}{2}\sigma_\tau^2\frac{\partial^2 m}{\partial s^2}\right)\frac{\partial f}{\partial m} + \tfrac{1}{2}\sigma_\tau^2\left(\frac{\partial m}{\partial s}\right)^2\frac{\partial^2 f}{\partial m^2}e^{2r_0\tau}\end{aligned} \tag{33}$$

With the definition of moneyness,

$$m_\tau = m(s_\tau,\tau) = \frac{S_t e^{r_0\tau} - x}{\sigma_0\sqrt{\tau}},$$

gives

$$\begin{aligned}\frac{\partial m}{\partial\tau} &= r_0 s_\tau\frac{1}{\sigma_0\sqrt{\tau}} - \tfrac{1}{2}\frac{m_\tau}{\tau} \\ \frac{\partial m}{\partial s} &= \frac{1}{\sigma_0\sqrt{\tau}} \\ \frac{\partial^2 m}{\partial s^2} &= 0.\end{aligned}$$

Inserting in (33) and multiplying with τ gives

$$(\tau\Delta r + \gamma)\,f = -\tau\frac{\partial f}{\partial\tau} + \left((\tau\Delta r + \tfrac{1}{2})m_\tau + \sqrt{\tau}\frac{\Delta r x}{\sigma_0}\right)\frac{\partial f}{\partial m} + \tfrac{1}{2}\frac{\sigma_\tau^2}{\sigma_0^2}\frac{\partial^2 f}{\partial m^2}e^{2r_0\tau} \tag{34}$$

where $\Delta r = r_\tau - r_0$ and

$$\gamma = \tau\frac{\partial g/\partial\tau}{g} = \begin{cases}\frac{1}{2} & \text{for} \quad g(\tau) = \sqrt{\tau} \qquad \text{(European)} \\ 0 & \text{for} \quad g(\tau) = 1 \qquad \text{(Binary)}\end{cases}$$

THE BLACK-SCHOLES MODEL

For the Black-Scholes setup, $\Delta r = 0$ and $\sigma_\tau = \sigma S_t = \sigma s_\tau\exp(-r\tau)$ and, as defined $\sigma_0 = \sigma x$. Inserting in (34) gives

$$\gamma f = -\frac{\partial f}{\partial\tau} + \tfrac{1}{2}m_\tau\frac{\partial f}{\partial m} + \tfrac{1}{2}(1+\sigma\sqrt{\tau}m_\tau)^2\frac{\partial^2 f}{\partial m^2}$$

since $S_\tau = (1+\sigma\sqrt{\tau}m_\tau)x\exp(-r_0\tau)$

E.2 TRANSFORMED PDE, BASED ON θ

Consider now the transformations:

$$\begin{aligned}
\theta &= \sqrt{\tau} = \sqrt{T-t}, \\
s_\theta &= S_t e^{r_0\theta^2}, \\
u(s_\theta,\theta) &= U(S_t,t)e^{r_0\theta^2}, \\
m_\theta &= \frac{s_\theta - x}{\sigma_0\theta}, \\
g(\theta)f(m_\theta,\theta) &= u(s_\theta,\theta),
\end{aligned}$$

where $r_0 = r(x,0)$ and $g(\theta)$ is known. Then

$$\begin{aligned}
\frac{\partial U}{\partial t} &= -\frac{\partial}{\partial\theta}g(\tau)f(m_\tau,\tau)e^{-r_0\tau}\frac{\partial\theta}{\partial t} \\
&= -\tfrac{1}{2}\frac{1}{\theta}\left(\frac{\partial g}{\partial\theta}f + g\frac{\partial f}{\partial\theta} + g\frac{\partial f}{\partial m}\frac{\partial m}{\partial\theta} - 2r_0\theta gf\right) - r_0\theta^2 \qquad \text{since} \qquad \frac{\partial\theta}{\partial t} = -\frac{\theta}{2} \\
&= -\tfrac{1}{2}\frac{1}{\theta}\left(\frac{\partial g}{\partial\theta}f + g\frac{\partial f}{\partial\theta} + g\frac{\partial f}{\partial m}\left(2\frac{r_0}{\sigma}s_\theta - \frac{m_\theta}{\theta}\right) - 2r_0\theta gf\right)e^{-r_0\theta^2}, \\
&\quad \text{since} \quad \frac{\partial m}{\partial\theta} = 2\frac{r_0}{\sigma}s_\theta - \frac{m_\theta}{\theta}, \\
\frac{\partial U}{\partial S} &= g\frac{\partial f}{\partial m}\frac{\partial m}{\partial s}\frac{\partial s}{\partial S}e^{-r_0\theta^2} \\
&= g\frac{\partial f}{\partial m}\frac{1}{\sigma_0\theta},
\end{aligned}$$

and

$$\begin{aligned}
\frac{\partial^2 U}{\partial S^2} &= g\frac{\partial^2 f}{\partial m^2}\left(\frac{\partial m}{\partial s}\right)^2\frac{\partial s}{\partial S} + g\frac{\partial f}{\partial m}\frac{\partial^2 m}{\partial s^2}\frac{\partial s}{\partial S} \\
&= g\frac{\partial^2 f}{\partial m^2}\frac{1}{(\sigma_0\theta)^2}e^{r_0\theta^2}.
\end{aligned}$$

Inserting in (32), multiplying with $1/g$, $\exp(r_0\theta^2)$, and θ^2 gives

$$\theta^2 r_\theta f = -\gamma f - \frac{\theta}{2}\frac{\partial f}{\partial\theta} - \left(\frac{\theta r_0 s_\theta}{\sigma_0} - \frac{m_\theta}{2}\right)\frac{\partial f}{\partial m} + \theta^2 r_0 f + \frac{\theta r_\theta s_\theta}{\sigma_0}\frac{\partial f}{\partial m} + \frac{e^{2r_0\theta^2}\sigma_\theta^2}{2\sigma_0^2}\frac{\partial^2 f}{\partial m^2}$$

(35) $\Downarrow$

$$(\theta^2\Delta r + \gamma)f = -\frac{\theta}{2}\frac{\partial f}{\partial\theta} + \left(\frac{\theta\Delta r x}{\sigma_0} + (\theta^2\Delta r + \tfrac{1}{2})m_\theta\right)\frac{\partial f}{\partial m} + e^{2r_0\theta^2}\frac{\sigma_\theta^2}{2\sigma_0^2}\frac{\partial^2 f}{\partial m^2}.$$

E.3 ASYMPTOTIC SOLUTION

To see that the two PDE's in (34) and (35) obey the limit conditions for the vanilla call in (30) and the binary call in (31), note that for $(m_\tau,\tau),(m_\tau,\tau) \to (x,0)$, $\Delta r \to 0$ and $\sigma_\tau,\sigma_\theta \to \sigma_0$. Hence, both (34) and (35) converges to

$$\gamma f = \tfrac{1}{2}m\frac{\partial f}{\partial m} + \tfrac{1}{2}\frac{\partial^2 f}{\partial m^2}$$

VANILLA CALL

Since $\gamma = \frac{1}{2}$ for the vanilla call, the initial condition $f_0(m)$ must obey

$$f = m\frac{\partial f}{\partial m} + \frac{\partial^2 f}{\partial m^2}. \tag{36}$$

According to (30)

$$f_0(m) = \sigma_0 \left(m\Phi(m) + \phi(m) \right).$$

The derivatives are easily determined as

$$\begin{aligned} \frac{\partial f_0}{\partial m} &= \sigma_0(\Phi(m) + m\phi(m) - m\phi(m)) \\ &= \sigma_0\Phi(m) \end{aligned}$$

and

$$\frac{\partial^2 f_0}{\partial m^2} = \sigma_0\phi(m).$$

And it is seen that f_0 obeys (36).

E.4 BINARY CALL

Since $\gamma = 0$ for the vanilla call, the initial condition $f_0(m)$ must obey

$$0 = m\frac{\partial f}{\partial m} + \frac{\partial^2 f}{\partial m^2}. \tag{37}$$

According to (31)

$$f_0(m) = \Phi(m).$$

The derivatives are easily determined as

$$\frac{\partial f_0}{\partial m} = \phi(m)$$

and

$$\frac{\partial^2 f_0}{\partial m^2} = -m\phi(m).$$

And it is seen that f_0 obeys (37).

APPENDIX F ALTERNATIVE MONEYNESS-DEFINITION

Consider the following alternative volatility-adjusted moneyness definition,

$$\begin{aligned} n(s_\tau, \tau) &= \frac{\log(s_t/x)}{\sigma_0\sqrt{\tau}} \\ &= \frac{\log(S_t/x) + r_0\tau}{\sigma_0\sqrt{\tau}}. \end{aligned}$$

To derive the appropriate PDE, note that

$$\begin{aligned}\frac{\partial n}{\partial \tau} &= r_0 \frac{1}{\sigma_0\sqrt{\tau}} - \tfrac{1}{2}\frac{n_\tau}{\tau} \\ \frac{\partial n}{\partial s} &= \frac{1}{s_\tau \sigma_0 \sqrt{\tau}} \\ \frac{\partial^2 n}{\partial s^2} &= -\frac{1}{s_\tau^2 \sigma_0 \sqrt{\tau}}.\end{aligned}$$

Inserting in (33) gives

$$\begin{aligned}\left(\Delta r + \frac{\gamma}{\tau}\right) f &= -\frac{\partial f}{\partial \tau} + \left(r_\tau s_\tau \frac{1}{s_\tau \sigma_0 \sqrt{\tau}} - \frac{r_0}{\sigma_0\sqrt{\tau}} + \tfrac{1}{2}\frac{n_\tau}{\tau} - \tfrac{1}{2}\sigma_\tau^2 \frac{1}{s_\tau^2 \sigma_0 \sqrt{\tau}} \right) \frac{\partial f}{\partial n} \\ &\qquad + \tfrac{1}{2}\sigma_\tau^2 \frac{1}{(s_\tau \sigma_0 \sqrt{\tau})^2} \frac{\partial^2 f}{\partial n^2} e^{2r_0\tau} \\ &= -\frac{\partial f}{\partial \tau} + \left(\frac{\Delta r}{\sigma_0\sqrt{\tau}} + \tfrac{1}{2}\frac{n_\tau}{\tau} - \tfrac{1}{2}\sigma_\tau^2 \frac{1}{s_\tau^2 \sigma_0 \sqrt{\tau}} \right) \frac{\partial f}{\partial n} \\ &\qquad + \tfrac{1}{2}\sigma_\tau^2 \frac{1}{(s_\tau \sigma_0 \sqrt{\tau})^2} \frac{\partial^2 f}{\partial n^2} e^{2r_0\tau}\end{aligned}$$

Multiplying with τ gives

$$\begin{aligned}(\tau \Delta r + \gamma) f &= -\tau \frac{\partial f}{\partial \tau} + \left(\sqrt{\tau}\frac{\Delta r}{\sigma_0} + \tfrac{1}{2} n_\tau - \tfrac{1}{2}\sqrt{\tau}\frac{\sigma_\tau^2}{s_\tau^2 \sigma_0} \right) \frac{\partial f}{\partial n} \\ &\qquad + \tfrac{1}{2}\frac{\sigma_\tau^2}{(s_\tau \sigma_0)^2} \frac{\partial^2 f}{\partial n^2} e^{2r_0\tau}\end{aligned}$$

with the limiting version, for $(s,\tau) \to (x,0)$, equal to

$$\gamma f = +\tfrac{1}{2} n_\tau \frac{\partial f}{\partial n} + \tfrac{1}{2}\frac{1}{x^2}\frac{\partial^2 f}{\partial n^2}. \tag{38}$$

In the special case of Black Scholes, $\Delta r = 0$, $\sigma_\tau = \sigma S_t = \sigma s_\tau \exp(-r\tau)$ and, according to the notation convention, $\sigma_0 = \sigma x$. The resulting PDE is

$$\gamma f = -\tau \frac{\partial f}{\partial \tau} + \left(\tfrac{1}{2} n_\tau - \tfrac{1}{2}\frac{\sigma\sqrt{\tau}}{x} e^{-2r_0\tau} \right) \frac{\partial f}{\partial m} + \tfrac{1}{2}\frac{1}{x^2}\frac{\partial^2 f}{\partial m^2}.$$

F.1 Initial Condition for a Vanilla Call

From Appendix B, the heat equation solution for the vanilla call in terms of s_τ is

$$\begin{aligned}u(s_\tau,\tau) &= (s_\tau - x)\Phi\left(\frac{s_\tau - x}{\sigma_0\sqrt{\tau}}\right) + \sigma_0\sqrt{t}\,\phi\left(\frac{s_\tau - x}{\sigma_0\sqrt{\tau}}\right) \\ &= \sqrt{\tau}\,\sigma_0\left(m_\tau \Phi(m_\tau) + \phi(m_\tau)\right), \qquad m_\tau = \frac{(e^{\sigma_0\sqrt{\tau}\,n_\tau} - 1)x}{\sigma_0\sqrt{\tau}}\end{aligned}$$

Where m_τ should be interpreted as a function of n_τ. To obtain the limit version as $(s,\tau) \to (x,0)$ note that L'Hospital´s gives

$$m_\tau \to n_\tau s_\tau \quad \text{for} \quad \tau \to 0.$$

Hence, the initial conditions for a vanilla call is given according to

$$u(s_\tau, \tau) = \sqrt{\tau}\ \sigma_0 \Big(n_\tau x \Phi(n_\tau x) + \phi(n_\tau x) \Big) \quad \text{for} \quad \tau \to 0.$$

To see that this equation fulfill (38) note that

$$\frac{\partial u}{\partial n} = \sqrt{\tau}\ \sigma_0 x \Phi(n_\tau x)$$

and

$$\frac{\partial^2 u}{\partial n^2} = \sqrt{\tau}\ \sigma_0 x^2 \phi(n_\tau x).$$

And the result follows by multiplying with n_τ, dividing by x^2, and by noting that $\gamma = \frac{1}{2}$ in the vanilla case.

F.2 Initial Condition for a Binary Call

From Appendix C, the heat equation solution for the binary call in terms of s_τ is

$$\begin{aligned} u(s_\tau, \tau) &= \Phi\left(\frac{s_\tau - x}{\sigma_0 \sqrt{\tau}} \right) \\ &= \Phi(m_\tau), \qquad\qquad m_\tau = \frac{(e^{\sigma_0 \sqrt{\tau}\ n_\tau} - 1)x}{\sigma_0 \sqrt{\tau}} \end{aligned}$$

Where m_τ should be interpreted as a function of n_τ. Using the results above gives initial conditions for a binary call,

$$u(s_\tau, \tau) = \Phi(n_\tau x) \qquad \text{for} \quad \tau \to 0$$

To see that this equation fulfill (38) note that

$$\frac{\partial u}{\partial n} = x \phi(n_\tau x)$$

and

$$\frac{\partial^2 u}{\partial n^2} = -n_\tau x^3 \phi(n_\tau x).$$

The result follows after multiplying with n_τ, dividing by x^2, and by noting that $\gamma = 0$ in the binary case.

References

Barone-Adesi, G., A. Bermudez, and J. Hatgioannides (2003): "Two-factor Convertible Bonds Valuation using the Method of Characteristics/Finite Elements," *Journal of Economic Dynamics and Control*, 27:1801–1831.

DE BOOR, C. (1978): *A Practical Guide to Splines,* Springer-Verlag.

FORSYTH, P. A., K. R. VETZAL, AND R. ZVAN (1999): "A Finite Element Approach to the Pricing of Discrete Lookbakcs with Stochastic Volatility," *Applied Mathematical Finance*, 6:87–106.

HESTON, S. AND G. ZHOU (2000): "On the Rate of Convergence of Discrete-time Contingent Claims," *Mathematical Finance*, 10(1):53–75.

JACKSON, N. AND E. SÜLI (1998): "Adaptive Finite Element Solution of 1D European Option Pricing Problems," Rapport 97/05, Oxford University Computing Laboratory, Oxford.

JUDD, K. L. (1998): *Numerical Methods in Economics,* MIT press.

KREISS, H., V. THOMÉE, AND O. WIDLUND (1970): "Smoothing of Initial Data and Rates of Convergence for Parabolic Difference Equations," *Communications on Pure and Applied Mathematics*, 23:241–259.

LAI, T. L. AND S. P.-S. WONG (2004): "Valuation of American Options via Basis Functions," *IEEE Transactions on Automatic Control*, 49(3):374–385.

POOLEY, D., P. FORSYTH, K. VETZAL, AND R. SIMPSON (2000): "Unstructured Meshing for two Asset Barrier Options," *Applied Mathematical Finance*, 7:33–60.

POOLEY, D. M., K. R. VETZAL, AND P. A. FORSYTH (2003): "Convergence Remedies for Non-smooth Payoffs in Option Pricing," *Journal of Computational Finance*, 6(4):25–40.

RANNACHER, R. (1984): "Finite Element Solution of Diffusion Problems with Irregular Data," *Numerische Mathematik*, 43:309–327.

RUST, J. (1994): "Estimation of Dynamic Structural Models: Problems and Prospects: Discrete Decision Processes," in Sims, C. and J. J. Laffont, editors, *Proceedings of the 6th World Congress of the Econometric Society, Barcelona, Spain*. Cambridge University Press.

TAVELLA, D. AND C. RANDALL (2000): *Pricing Financial Instruments: The Finite Difference Method,* John Wiley & Sons, Inc., New York.

THOMÉE, V. AND L. B. WAHLBIN (1974): "Convergence Rates of Parabolic Difference Schemes for Non-smooth data," *Mathematics of Computation*, 28(125):1–13.

WILMOTT, P., J. DEWYNNE, AND HOWISON (1993): *Option Pricing: Mathematical Models and Computation,* Oxford Financial Press, Oxford.

ZVAN, R., P. A. FORSYTH, AND K. R. VETZAL (1998a): "Penalty Methods for American Options with Stochastic Volatility," *Journal of Computational and Applied Mathematics,* 91:199–218.

——— (1998b): "Robust Numerical Methods for PDE Models of Asian Options," *Journal of Computational Finance,* 1(2):39–78.

——————— (1999): "Discrete Asian Barrier Options," *Journal of Computational Finance*, 3(1):41–68.

——————— (2000): "PDE Methods for Pricing Barrier Options," *Journal of Economic Dynamics and Control*, 24:1563–1590.

——————— (2001): "A Finite Volume Approach for Contingent Claims Valuation," *IMA Journal of Numerical Analysis*, 21:703–731.

INSTITUT FOR FINANSIERINGs working papers siden 2000:

WP 2000-1 Bjarne Astrup Jensen and Carsten Sørensen: Paying for minimum interest rate guarantees: Who should compensate who?

WP 2000-2 Jan Jakobsen and Ole Sørensen: Decomposing and testing Long-run Returns with an application to initial public offerings in Denmark.

WP 2000-3 Jan Jakobsen and Torben Voetmann: Volatility-Adjusted Performance An Alternative Approach to Interpret Long-Run Returns.

WP 2000-4 Jan Jakobsen and Torben Voetmann: Post-Acquisition Performance in the Short and Long-Run Evidence from the Copenhagen Stock Exchange 1993-1997.

WP 2000-5 Ken L. Bechmann and Johannes Raaballe: A Regulation of Bids for Dual Class Shares. Implication: Two Shares – One Price.

WP 2000-6 Torben Voetmann: Changes in the Bid-Ask Componets Around Earnings Announcemtents: Evidence from the Copenhagen Stock Exchange.

WP 2000-7 Henrik Lando: The Optimal Standard of Proof in Criminal Law When Both Fairness and Deterrence Are Social Aims.

WP 2000-8 Jesper Rangvid and Carsten Sørensen: Convergence in the ERM and Declining Numbers of Common Stochastic Trends.

WP 2000-9 Claus Munk and Carsten Sørensen: Optimal Consumption and Investment Strategies with Stochastic Interest Rates.

WP 2000-10 Henrik Lando and Caspar Rose: On Specific Performance in Civil Law and Enforcement Costs.

WP 2000-11 Henrik Lando: Ny lov om jordforurening i økonomisk belysning.

WP 2001-1 Michael Møller, Claus Parum og Thomas Sørensen: Den ny pensionsafkastbeskatningslov.

WP 2001-2 Bjarne Astrup Jensen: Mean variance efficient portfolios by linear programming: A review of some portfolio selection criteria of Elton, Gruber and Padberg.

WP 2001-3 Caspar Rose: Impact of Investor Meetings/Presentations on Share

Prices, Insider Trading and Securities Regulation.

WP 2001-4 Caspar Rose: Corporate Financial Performance and the Use of Takeover Defenses.

WP 2001-5 Shubhashis Gangopadhyay and Clas Wihlborg: The Impact of Bankruptcy Rules on Risky Project Choice and Skill Formation under Credit Rationing.

WP 2001-6 Claus Munk, Carsten Sørensen & Tina Nygaard Vinther: Portfolio Choice under Inflation: Are Popular Recommendations Consistent with Rational Behaviour?

WP 2001-7 Ken L. Bechmann: Evidence on the Limits of Arbitrage: Short Sales, Price Pressure, and the Stock Price Response to Convertible Bond Calls.

WP 2001-8 Michael Møller & Caspar Rose: Legal pre-emption rights as call-options, redistribution and efficiency loss.

WP 2001-9 Peter Raahauge: Empirical Rationality in the Stock Market.

WP 2002-1 Bjarne Astrup Jensen: On valuation before and after tax in no arbitrage models: Tax neutrality in the discrete time model.

WP 2002-2 Ken L. Bechmann: Price and Volume Effects Associated with Changes in the Danish Blue-Chip Index – The KFX Index.

WP 2002-3 Steen Thomsen and Caspar Rose: Foundation ownership and financial performance. Do companies need owners?

WP 2002-4 Martin Richter and Carsten Sørensen: Stochastic Volatility and Seasonality in Commodity Futures and Options: The Case of Soybeans.

WP 2002-5 Caspar Rose: Aktiemarkedets reaktion på indførelsen af incitaments-programmer.

WP 2002-6 Caspar Rose: Impact of Takeover Defenses on Managerial Incentives.

WP 2002-7 Ken L. Bechmann og Peter Løchte Jørgensen: Optionsaflønning i danske børsnoterede selskaber.

WP 2002-8 Jesper Rangvid: Output and Expected Returns – a multicountry study.

WP 2002-9 Jonas Aziz Bhatti og Michael Møller: Pensionsafkastbeskatning og optimal porteføljesammensætning.

WP 2003-1	Bjarne Florentsen, Michael Møller and Niels Chr. Nielsen: Reimbursement of VAT on written-off Receivables.
WP 2003-2:	Ken L. Bechmann and Peter Løchte Jørgensen: The Value and Incentives of Option-based Compensation in Danish Listed Companies.
WP 2004-1	Ken L. Bechmann and Johannes Raaballe: The Difference Between Stock Splits and Stock Dividends – Evidence from Denmark.
WP 2004-2	Caspar Rose: Bestyrelsessammensætning og finansiel performance i danske børsnoterede virksomheder - Er Nørbyrapportens anbefalinger til gavn for aktionærerne?
WP 2004-3	Jens Lunde: Lack of balance in after-tax returns - lack of tenure neutrality. The Danish case.
WP 2004-4	Peter Raahauge: Upper Bounds on Numerical Approximation Errors.
WP 2004-5	Peter Raahauge: Higher-Order Finite Element Solutions of Option Prices.